

1 **Sex-Specific Evolution of the Genome-wide Recombination**  
2 **Rate**

3 April L. Peterson, Bret A. Payseur

University of Wisconsin-Madison, Laboratory of Genetics

Submission to eLife

Subject: Evolutionary Biology

Senior Editors: Patricia Wittkopp, Diethard Tautz

Reviewing Editors: Graham Coop, Molly Przeworski

4

## 5 ABSTRACT

6 Although meiotic recombination is required for successful gametogenesis in most species  
7 that reproduce sexually, the rate of crossing over varies among individuals. Differences in  
8 recombination rate between females and males are perhaps the most striking form of this  
9 variation. To determine how sex shapes the evolution of recombination, we directly  
10 compared the genome-wide recombination rate in females and males across a common set  
11 of genetic backgrounds in house mouse. Our results reveal highly discordant evolutionary  
12 trajectories in the two sexes. Whereas male recombination rates show rapid evolution over  
13 short timescales, female recombination rates measured in the same strains are mostly  
14 static. Strains with high recombination in males have more double-strand breaks and  
15 stronger crossover interference than strains with low recombination in males, suggesting  
16 that these factors contribute to the sex-specific evolution we document. Our findings  
17 provide the strongest evidence yet that sex is a primary driver of recombination rate  
18 evolution.

## 20 INTRODUCTION

21 Meiosis converts diploid germ cells into haploid gametes. During meiosis I, DNA crossovers  
22 aid the separation of homologous chromosomes by physically linking them and  
23 establishing tension between them on the spindle (Petronczki et al., 2003). The wrong  
24 number of recombination events can disrupt chromosomal segregation, leading to  
25 infertility, miscarriage, and birth defects (Hassold and Hunt, 2001). Recombination also  
26 shapes evolution by shuffling the combinations of genetic variants offspring inherit.  
27 Recombination affects the fates of beneficial and deleterious mutations (Felsenstein, 1974;  
28 Fisher, 1930; Hill and Robertson, 1966) and interacts with natural selection to leave  
29 gradients in genomic patterns of diversity (Begun and Aquadro, 1992; Charlesworth et al.,  
30 1993; Cutter and Payseur, 2013; Nachman and Payseur, 2012; Smith and Haigh, 1974).

The role of recombination in facilitating meiotic chromosome assortment suggests that the total number of crossovers in a cell – the genome-wide recombination rate – is an important cellular characteristic connected to organismal fitness. The dual pressures of ensuring at least one crossover per chromosome and minimizing levels of DNA damage and ectopic exchange are thought to impose lower and upper thresholds on the genome-wide recombination rate (Inoue and Lupski, 2002; Nagaoka et al., 2012). Yet, within these bounds, individuals from the same species can vary substantially in crossover number (Gruhn et al., 2013; Johnston et al., 2016; Kong et al., 2008; Ma et al., 2015).

Sex is perhaps the most notable axis along which recombination rate varies. Broadly speaking, sexual dimorphism in the genome-wide recombination rate assumes two forms. In species such as *Drosophila melanogaster*, one sex completes meiosis without forming crossovers (“achiasmy”), while the other sex recombines (Burt et al., 1991; Haldane, 1922; Huxley, 1928). Alternatively, in most species with recombination, crossovers occur in both sexes but at different rates (“heterochiasmy”). In these species, females tend to recombine more than males (Bell, 1982; Brandvain and Coop, 2012; Burt et al., 1991; Lenormand and Dutheil, 2005; Lorch, 2005). In plants, heterochiasmy is correlated with the opportunity for haploid selection (Lenormand and Dutheil, 2005).

Despite the establishment of these interspecific trends, an understanding of how sex shapes the evolution of recombination cannot be achieved with available data. Comprehensive comparisons of variation in female and male recombination rates within species have come from outbred populations of humans (Gruhn et al., 2013; Halldorsson et al., 2019; Kong et al., 2004, 2014, 2008), dog (Campbell et al., 2016), cattle (Ma et al., 2015; Shen et al., 2018), and Soay sheep (Johnston et al., 2016), in which the role of sex is confounded with the contributions of genetic variation. Although it is known that the level and direction of heterochiasmy can differ among species (Brandvain and Coop, 2012; Lenormand and Dutheil, 2005), the correlation between female and male recombination rates among closely related species remains poorly documented. Direct contrasts between the two sexes across a common, diverse set of genomic backgrounds that represent recent timescales would reveal whether the genome-wide recombination rate evolves differently in males and females.

Examining variation in the total number of crossovers in a sex-specific manner could also illuminate evolutionary connections between recombination rate and crossover positioning. Analyses of meiotic chromosome morphology in *Arabidopsis thaliana*, *Caenorhabditis elegans*, and *Mus musculus* suggest that the sex with more recombination usually has longer chromosome axes (Cahoon and Libuda, 2019). A survey of 51 species found conserved sex differences in the recombination landscape, including telomere-biased placement of crossovers in males but not in females (Sardell and Kirkpatrick, 2020). The degree to which a crossover reduces the probability of another crossover nearby (crossover interference) also differs between females and males (Otto and Payseur, 2019).

The house mouse, *Mus musculus*, is a compelling system for understanding how sex affects the evolution of recombination. Multiple subspecies share a most recent common ancestor approximately 0.5 million years ago (Geraldes et al., 2011), providing the opportunity to examine natural variation on recent evolutionary timescales. Wild *Mus musculus* belong to the same species as classical inbred strains of mice, where the molecular and cellular pathways that lead to crossovers have been studied extensively (Baudat et al., 2013; Bolcun-Filas and Schimenti, 2012; Handel and Schimenti, 2010). Single-cell immunofluorescent approaches make it possible to estimate genome-wide recombination rates in individual males and females (Koehler et al., 2002; Peters et al., 1997). A collection of wild-derived inbred strains founded from a variety of geographic locations is available, enabling genetic variation in recombination to be profiled across the species range. Most importantly, by measuring recombination rates in females and males from the same set of wild-derived inbred strains, the evolutionary dynamics of recombination can be directly compared in the two sexes.

In this paper, we report genome-wide recombination rates from both sexes in a diverse panel of wild-derived inbred strains of house mice and their close relatives. We demonstrate that recombination rate evolves differently in females and males, even over short timescales.

## RESULTS

### Genome-wide recombination rate evolves differently in females and males

We used counts of MLH1 foci per cell to estimate genome-wide recombination rates in 14 wild-derived inbred strains sampled from three subspecies of house mice (*M. musculus domesticus*, *M. m. musculus* and *M. m. molossinus*) and three other species of *Mus* (*M. spretus*, *M. spicilegus*, and *M. caroli*). Mean MLH1 focus counts for 188 mice were quantified from an average of 21.77 spermatocytes per male (for a total of 1,742 spermatocytes) and 17.85 oocytes per female (for a total of 1,427 oocytes) (Table 1).

Graphical comparisons reveal sex-specific dynamics to the evolution of genome-wide recombination rate (Figure 1A). First, MLH1 focus counts differ between females and males in most strains. Second, the difference in counts between the sexes varies among strains. Although most strains show more MLH1 foci in females, two strains (*musculus*<sup>PWD</sup> and *molossinus*<sup>MSM</sup>) exhibit higher counts in males. In females, numbers of MLH1 foci are evenly distributed around the sex-wide mean of approximately 25 (Figure 1B). In stark contrast, males largely separate into two groups of strains with high numbers (near 30) and low numbers (near 23) of foci (Figure 1C). Strain mean MLH1 focus counts from females and males are uncorrelated (Spearman's  $\rho = 0.08$ ;  $p = 0.84$ ) across the set of strains.

To further partition variation in recombination rate, we fit a series of linear models to mean MLH1 focus counts from 137 house mice from *M. m. domesticus*, *M. m. musculus* and *M. m. molossinus* (Table 2; detailed results available in Supplemental Tables 1-7). Strain, sex, subspecies, and sex\*subspecies each affect MLH1 focus count in a linear mixed model (M1; strain (random effect):  $p < 10^{-4}$ ; sex:  $p = 3.64 \times 10^{-6}$ ; subspecies:  $p = 9.69 \times 10^{-4}$ ; subspecies\*sex:  $p = 1.8 \times 10^{-4}$ ).

The effect of subspecies is no longer significant in a model treating all factors as fixed effects (M2; *musculus*  $p = 0.24$ , *molossinus*  $p = 0.1$ ), highlighting strain and sex as salient variables. Two strains exhibit strong effects on MLH1 focus count (M3; *domesticus*<sup>G</sup>  $p = 1.78$

$\times 10^{-6}$ ; *domesticus*<sup>LEW</sup>  $p = 0.02$ ), with sex-strain interactions involving three strains (M3; *domesticus*<sup>G</sup>  $p < 10^{-6}$ ; *molossinus*<sup>MSM</sup>  $p < 10^{-6}$ ; *musculus*<sup>PWD</sup>  $p = 3.87 \times 10^{-4}$ ).

In separate analyses of males (M4;  $n = 71$ ), three strains disproportionately shape MLH1 focus count (as observed in Figure 1C): *musculus*<sup>PWD</sup> ( $p = 3.6 \times 10^{-7}$ ; effect = 6.11 foci, *molossinus*<sup>MSM</sup> ( $p = 6.3 \times 10^{-9}$ ; effect = 6.91), and *musculus*<sup>SKIVE</sup> ( $p = 8.22 \times 10^{-4}$ ; effect = 4.04). These three strains point to substantial evolution in the genome-wide recombination rate in spermatocytes; we subsequently refer to them as “high-recombination” strains. In females (M4;  $n = 76$ ), three strains affect MLH1 focus count: *domesticus*<sup>G</sup> ( $p = 8.7 \times 10^{-6}$ ; effect = 3.3), *molossinus*<sup>MSM</sup> ( $p = 2.43 \times 10^{-5}$ ; effect = 2.99), and *domesticus*<sup>LEW</sup> ( $p = 0.03$ ; effect = 1.69). Strain effect sizes in females are modest in magnitude compared to those in males. Together, these results demonstrate that the genome-wide recombination rate evolves in a highly sex-specific manner.

## Synaptonemal complexes are longer in females

The variation in sex differences in recombination we discovered provided an opportunity to determine whether sex differences in chromatin compaction, as measured by the length of the synaptonemal complex (SC), are reversed when heterochiasmy is reversed. In all strains except *musculus*<sup>SKIVE</sup>, females have longer SCs than males, whether SC length was estimated as the total length across bivalents or as the length of short bivalents (t-tests; all  $p < 0.05$ , except short bivalents in *musculus*<sup>SKIVE</sup>,  $p = 0.11$ ). Among short bivalents (to which the female X bivalent does not contribute), female to male ratios of mouse mean SC length range from 1.26 (*musculus*<sup>PWD</sup>) to 1.52 (*domesticus*<sup>WSB</sup>) across strains. That females have longer SCs is further supported by models that include covariates, which identify sex as the most consistently significant effect for total SC length (M1:  $p = 2.56 \times 10^{-31}$ ; M2:  $p = 2.56 \times 10^{-8}$ ; M3:  $p = 2.56 \times 10^{-8}$ ) (Supplemental Tables 8-14) and short bivalent SC length (M1:  $p = 1.12 \times 10^{-11}$ ; M2:  $p < 10^{-6}$ ; M3:  $p < 1.33 \times 10^{-7}$ ) (Supplemental Tables 15-21). The existence of some subspecies and strain effects on total SC length and short bivalent SC length further indicates that SC length has evolved among strains and among subspecies.

In summary, two approaches for measuring SC length demonstrate that females have longer SCs (chromosome axes), even in strains in which males recombine more. This pattern implies that in high-recombination strains, spermatocytes have less space than oocytes in which to position additional crossovers.

## **Females and males differ in crossover positions and crossover interference**

We used normalized positions of MLH1 foci along bivalents with a single focus to compare crossover location while controlling for differences in SC length. In all strains, MLH1 foci tend to be closer to the telomere in males (mean normalized position in males: 0.68; mean normalized position in females: 0.56; paired t-test;  $p = 8.49 \times 10^{-4}$ ). Sex is also the strongest determinant of MLH1 focus position in the models we tested (M1:  $p = 2.82 \times 10^{-26}$ ; M2:  $p = 3.96 \times 10^{-8}$ ; M3:  $p = 3.96 \times 10^{-8}$ ) (Supplemental Tables 24-30).

Males have longer normalized mean inter-focal distances (IFD<sub>norm</sub>) than females in seven out of eight strains (t-tests;  $p < 0.05$ ), with only *musculus*<sup>KAZ</sup> showing no difference ( $p = 0.33$ ). Examination of IFD<sub>norm</sub> distributions indicates that females are centered at approximately 50% and show a slight enrichment of low (<25%) values, whereas males are enriched for higher values. Models treating IFD<sub>norm</sub> as the dependent variable support the inference of stronger interference in males, with sex being the most significant variable (M1:  $p = 9.08 \times 10^{-12}$ ; M2:  $p = 0.01$ ; M3:  $p = 0.01$ ) (Supplemental Tables 34-37). In contrast, there is no clear signal of sex differences in raw mean inter-focal distances (IFD<sub>raw</sub>) (Supplemental Tables 38-40) across the full set of strains, whether they are considered separately or together. Visualization of normalized MLH1 foci positions on bivalents with two crossovers (Figure 3; Supplemental Figure 3) further suggests that interference distances vary more in females than in males, and that males display a stronger telomeric bias in the placement of the distal crossover.

In summary, controlling for differences in SC length (chromatin compaction) indicates that interference is consistently stronger in males, whereas interference on the physical scale is similar in the two sexes.

## Evolution of genome-wide recombination rate is dispersed across bivalents, associated with double-strand break number, and connected to crossover interference

We used the contrast between males from high-recombination strains and males from low-recombination strains to identify features of the recombination landscape associated with evolutionary transitions in the genome-wide recombination rate. We considered proportions of bivalents with different numbers of crossovers, double-strand break number, SC length, and crossover positioning.

Ninety-six percent of single bivalents in our pooled dataset ( $n = 9,569$ ) have either one or two MLH foci (Supplemental Figure 2). The proportions of single-focus (1CO) bivalents vs. double-focus (2CO) bivalents distinguish high-recombination strains from low-recombination strains (Supplemental Figure 2). High-recombination strains are enriched for 2CO bivalents at the expense of 1CO bivalents: proportions of 2CO bivalents are 0.33 in *musculus*<sup>SKIVE</sup>, 0.44 in *musculus*<sup>PWD</sup>, and 0.51 in *molossinus*<sup>MSM</sup> (Supplemental Figure 3). Following patterns in the genome-wide recombination rate, male *musculus*<sup>PWD</sup> and male *molossinus*<sup>MSM</sup> have 2CO proportions that are more similar to each other than to strains from their own subspecies (chi-square tests; *musculus*<sup>PWD</sup> vs. *molossinus*<sup>MSM</sup>:  $p = 0.37$ ; *musculus*<sup>PWD</sup> vs. *musculus*<sup>KAZ</sup>:  $p = 1.23 \times 10^{-31}$ ; *molossinus*<sup>MSM</sup> vs. *molossinus*<sup>MOLF</sup>:  $p = 2.34 \times 10^{-6}$ ). These results demonstrate that evolution of the genome-wide recombination rate reflects changes in crossover number across multiple bivalents.

To begin to localize evolution of genome-wide recombination rate to steps of the recombination pathway, we counted DMC1 foci in prophase spermatocytes as markers for double-strand breaks (DSBs). DMC1 foci were counted in a total of 76 early zygotene and 75 late zygotene spermatocytes from two high-recombination strains (*musculus*<sup>PWD</sup> and *molossinus*<sup>MSM</sup>) and three low-recombination strains (*musculus*<sup>KAZ</sup>, *domesticus*<sup>WSB</sup>, and *domesticus*<sup>G</sup>) (Table 3). High-recombination strains have significantly more DMC1 foci than low-recombination strains in early zygotene cells (t-test;  $p < 10^{-6}$ ). In contrast, the two strain groups do not differ in DMC1 foci in late zygotene cells (t-test;  $p = 0.66$ ). Since DSBs



are repaired as either COs or non-crossovers (NCOs), the ratio of MLH1 foci to DMC1 foci can be used to estimate the proportion of DSBs designated as COs. High-recombination and low-recombination strains do not differ in the MLH1/DMC1 ratio, whether DMC1 foci were counted in early zygotene cells or late zygotene cells (t-test;  $p > 0.05$ ). These results raise the possibility that the evolution of genome-wide recombination rate is primarily determined by processes that precede the CO/NCO decision, at least in house mice.

Total SC length only partially differentiates high-recombination strains from low-recombination strains (Figure 3). Whereas high-recombination strains as a group have significantly greater total SC length than low-recombination strains (t-test;  $p = 0.01$ ), separate tests within subspecies show that the two strain categories differ within *M. m. molossinus* ( $p = 2.59 \times 10^{-4}$ ) but not within *M. m. musculus* ( $p = 0.65$ ). Additionally, mouse means for the reduced (short and long) bivalent datasets do not differ between high-recombination and low-recombination strains (t-test; short:  $p = 0.84$ ; long:  $p = 0.19$ ). In a model with total SC length as the dependent variable (M4), the two subspecies effects are significant (*M. m. musculus*  $p = 3.95 \times 10^{-7}$ ; *M. m. molossinus*  $p = 3.33 \times 10^{-7}$ ), but there are also strain-specific effects (Supplemental Table 13). In models with SC lengths of short and long bivalents as dependent variables, several subspecies and strain effects reach significance ( $p < 0.05$ ) (Supplemental Table 20,21, 22, and 23), but they are not consistent across models. Collectively, these results reveal that evolution of SC length is not strongly associated with evolution of genome-wide recombination rate in house mice.

In summary, evolution of the genome-wide recombination rate in males is connected to double-strand break number and crossover interference, but not to SC length and crossover position (on single-crossover bivalents).

## DISCUSSION

By comparing recombination rates in females and males from the same diverse set of genetic backgrounds, we isolated sex as a primary factor in the evolution of this fundamental meiotic trait. Recombination rate differences are more pronounced in males than females. Because inter-strain divergence times are identical for the two sexes, this

observation demonstrates that the genome-wide recombination rate evolves faster in males. More generally, recombination rate divergence is decoupled in females and males. These disparities are remarkable given that recombination rates for the two sexes were measured in identical genomic backgrounds (other than the number and identity of sex chromosomes). Our results provide the strongest evidence yet that the genome-wide recombination rate follows distinct evolutionary trajectories in males and females.

At the genetic level, the sex-specific patterns we documented indicate that some mutations responsible for the evolution of recombination rate have dissimilar phenotypic effects in the two sexes. A subset of the genetic variants associated with genome-wide recombination rate within populations of humans (Kong et al., 2004, 2008, 2014; Halldorsson et al., 2019), Soay sheep (Johnston et al., 2016), and cattle (Ma et al., 2015; Shen et al., 2018) appear to show sex-specific properties, including opposite effects in females and males. Furthermore, inter-sexual correlations for recombination rate are weak in humans (Fledel-Alon et al., 2011) and Soay sheep (Johnston et al., 2016). Crosses between the strains we surveyed could be used to identify and characterize the genetic variants responsible for recombination rate evolution in house mice (Dumont and Payseur, 2011; Wang et al., 2019; Wang and Payseur, 2017). These variants could differentially affect females and males at any step in the recombination pathway. Although our DMC1 profiling was limited to males from a small number of strains (for practical reasons), our findings suggest that mutations that determine the number of double-strand breaks contribute to sex-specific evolution in the recombination rate. A study of two classical inbred strains and one wild-derived inbred strain of house mice also found a positive association between crossover number and double-strand break number in males (Baier et al., 2014).

Another implication of our results is that the connection between recombination rate and fitness differs between males and females. Little is known about whether and how natural selection shapes recombination rate in nature (Dapper and Payseur, 2017; Ritz et al., 2017). Samuk et al. (2020) recently used a quantitative genetic test to conclude that an 8% difference in genome-wide recombination rate between females from two populations of *Drosophila pseudoobscura* was caused by natural selection. Applying similar strategies to

species in which both sexes recombine, including house mice, would be a logical next step to understanding the sex-specific evolution of recombination rate.

Population genetic models have been built to explain sexual dimorphism in the number and placement of crossovers, which is a common phenomenon (Brandvain and Coop, 2012; Sardell and Kirkpatrick, 2020). Modifier models predicted that lower recombination rates in males will result from haploid selection (Lenormand, 2003) or sexually antagonistic selection on coding and cis-regulatory regions of genes (Sardell and Kirkpatrick, 2020). Another modifier model showed that meiotic drive could stimulate female-specific evolution of the recombination rate (Brandvain and Coop, 2012). Although these models fit the conserved pattern of sex differences in crossover positions, they do not readily explain our observations of sex-specific evolution in the genome-wide recombination rate. In particular, the alternation across strains in which sex has more crossovers is unexpected.

We propose an alternative interpretation of our findings based on the cell biology of gametogenesis. During meiosis, achieving a stable chromosome structure requires the attachment of kinetochores to opposite poles of the cell and at least one crossover to create tension across the sister chromosome cohesion distal to chiasmata (Dumont and Desai, 2012; Lane and Kauppi, 2019; Subramanian and Hochwagen, 2014; VanVeen and Hawley, 2003). The spindle assembly checkpoint (SAC) prevents aneuploidy by ensuring that all bivalents are correctly attached to the microtubule spindle (“bi-oriented”) before starting the metaphase-to-anaphase transition via the release of the sister cohesion holding homologs together (Lane and Kauppi, 2019). Hence, selection seems likely to favor mutations that optimize the process of bi-orientation and chromosome separation, thereby prohibiting the SAC from delaying the cell cycle or triggering apoptosis. Multiple lines of evidence indicate that the SAC is more effective in spermatogenesis than in oogenesis (Lane and Kauppi, 2019), perhaps due to the presence of the acentrosome spindle (So et al., 2019) and larger cell volume (Kyogoku and Kitajima, 2017) in oocytes. The higher stringency of the SAC during spermatogenesis suggests that selection will be better at removing mutations that interfere with bi-orientation in males than in females. Therefore, faster male evolution of the genome-wide recombination rate could be driven by the more stringent SAC acting on chromosome structures at the metaphase I alignment.

Our SAC model is consistent with other features of our data. We showed that widespread sex differences in broad-scale crossover positioning (Sardell and Kirkpatrick, 2020) apply across house mice, even in lineages where the direction of heterochiasmy is reversed. Faster spermatogenesis may select for synchronization of the separation across all homologs within the cell (Kudo et al., 2009), whereas in oogenesis, the slower cell cycle and multiple arrest stages may require chromosome structures with greater stability on the meiosis I spindle, especially for those organisms that undergo dictyate arrest (Lee, 2019).

We propose that the SAC model also can explain the correlated evolution of stronger crossover interference and higher genome-wide recombination rate in male house mice. Our results show that crossovers are spaced further apart in strains enriched for double-crossover bivalents when SC length is considered and bivalent size effects are minimized. Assuming chromatin compaction between (prophase) pachytene and metaphase is uniform along bivalents, this increased spacing is expected to expand the area for sister cohesion to connect homologs and may improve the fidelity of chromosomal segregation. While the SAC model postulates direct fitness effects of interference, a modifier model predicted that indirect selection on recombination rate – via its modulation of offspring genotypes – can strengthen interference as well (Goldstein et al., 1993).

Regardless of the underlying mechanism, our results provide a rare demonstration that crossover interference can diverge over short evolutionary timescales. The notion that stronger interference can co-evolve with higher genome-wide recombination rate is supported by differences between breeds of cattle (Ma et al., 2015). In contrast, mammalian species with stronger interference tend to exhibit lower genome-wide recombination rates (Otto and Payseur, 2019; Segura et al., 2013). The evolution of crossover interference and its relationship to changes in crossover number on the genomic scale is a topic deserving of more empirical and theoretical work.

Our findings further reveal that evolution of the genome-wide recombination rate does not require major changes in the degree of chromatin compaction. Female house mice consistently show longer SCs, even in strains with more recombination in males. Studies in mice (Lynn et al., 2002; Petkov et al., 2007) and humans (Gruhn et al., 2013; Tease and

Hulten, 2004) suggest that chromosomal axes are longer (and DNA loops are shorter) in females than males. Some authors have suggested that conserved sex differences in crossover positioning (more uniform placement in females) and interference strength (stronger interference in males) could be due to looser chromatin packing of the meiotic chromosome structure in females (Haenel et al., 2018; Petkov et al., 2007). A cellular model designed to explain interference attributes sexual dimorphism in chromatin structure to greater cell volumes and oscillatory movements of telomeres and kinetochores in oocytes (Hultén, 2011). Recent work in mice connects the sparser recombination landscape in females to sex differences in crossover maturation efficiency (Wang et al., 2017).

Our conclusions are accompanied by several caveats. First, MLH1 foci only identify interfering crossovers (Holloway et al., 2008). Although most crossovers belong to this class (Holloway et al., 2008), our approach likely underestimated genome-wide recombination rates. Evolution of the number of non-interfering crossovers is a subject worth examining. A second limitation is that our investigation of crossover locations was confined to the relatively low resolution possible with immunofluorescent cytology. Positioning crossovers with higher resolution could reveal additional evolutionary patterns. Finally, the panel of inbred lines we surveyed may not be representative of recombination rate variation within and between subspecies of house mice. We considered most available wild-derived inbred lines, but house mice have a broad geographic distribution. Nevertheless, we expect our primary conclusion that recombination rate evolves in a sex-specific manner to be robust to geographic sampling because differences between females and males exist for the same set of inbred strains.

While the causes of sex differences in recombination remain mysterious (Lenormand et al., 2016), our conclusions have implications for a wide range of recombination research. For biologists uncovering the cellular and molecular determinants of recombination, our results suggest that mechanistic differences between the sexes could vary by genetic background. For researchers charting the evolutionary trajectory of recombination, our findings indicate that sex-specific comparisons are crucial. For theoreticians building evolutionary models of recombination, different fitness regimes and genetic architectures in females and males should be considered. Elevating sex as a primary determinant of

recombination would be a promising step toward integrating knowledge of cellular mechanisms with evolutionary patterns to understand recombination rate variation in nature.

## MATERIALS AND METHODS

### Mice

We used a panel of wild-derived inbred strains of house mice (*Mus musculus*) and related murid species to profile natural genetic variation in recombination (Table 4). Mice from the same inbred strain served as biological replicates. Our survey included 5 strains from *M. m. musculus*, 4 strains from *M. m. domesticus*, 2 strains from *M. m. molossinus*, 2 strains from *M. m. castaneus*, and 1 strain each from *M. spicilegus*, *M. spretus* and *M. caroli*. We subsequently denote strains by their abbreviated subspecies and name (*e.g. domesticus*<sup>WSB</sup>).

Mice were housed at dedicated, temperature-controlled facilities in the UW-Madison School of Medicine and Public Health, with the exception of mice from Gough Island, which were housed in a temperature-controlled facility in the UW-Madison School of Veterinary Medicine. Mice were sampled from a partially inbred strain of Gough Island mice, after approximately 6 generations of brother-sister matting. All mice were provided with *ad libitum* food and water. Procedures followed protocols approved by IACUC.

### Tissue Collection and Immunohistochemistry

The same dry-down spread technique was applied to both spermatocytes and oocytes, following Peters et al. (1997), with adjustment for volumes. Spermatocyte spreads were collected and prepared as described in Peterson et al. (2019). The majority of mice used for MLH1 counts were between 5 and 12 weeks of age. Juvenile males between 12 and 15 days of age were used for DMC1 counts. Both ovaries were collected from embryos (16-21 embryonic days) or neonates (0-48 hours after birth). Whole testes were incubated in 3ml of hypotonic solution for 45 minutes. Decapsulated ovaries were incubated in 300ul of hypotonic solution for 45 minutes. Fifteen microliters of cell slurry (masticated gonads)

were transferred to 80ul of 2% PFA solution. Cells were fixed in this solution and dried in a humid chamber at room temperature overnight. The following morning, slides were treated with a Photoflow wash (Kodak, diluted 1:200). Slides were stored at -20°C if not stained immediately. To visualize the structure of meiotic chromosomes, we used antibody markers for the centromere (CREST) and lateral element of the synaptonemal complex (SC) (SYCP3). Crossovers (COs) were visualized as MLH1 foci. Double strand breaks (DSBs) were visualized as DMC1 foci. The staining protocol followed (Anderson et al., 1999) and (Koehler et al., 2002). Antibody staining and slide blocking were performed in 1X antibody dilution buffer (ADB) (normal donkey serum (Jackson ImmunoResearch), 1X PBS, bovine serum albumin (Sigma), and Triton X-100 (Sigma)). Following a 30-minute blocking wash in ABD, each slide was incubated with 60ul of a primary antibody master mix for 48 hours at 37°C. The master mix recipe contained polyclonal anti-rabbit anti-MLH1 (Calbiochem; diluted 1:50) or anti-rabbit anti-DMC1 (mix of DMC1), anti-goat polyclonal anti-SYCP3, (Abcam; diluted 1:50), and anti-human polyclonal antibody to CREST (Antibodies, Inc; diluted 1:200) suspended in ADB. Slides were washed twice in 50ml ADB before the first round of secondary antibody incubation for 12 hours at 37°C. Alexa Fluor 488 donkey anti-rabbit IgG (Invitrogen, location; diluted to 1:100) and Coumarin AMCA donkey anti-human IgG (Jackson ImmunoResearch; diluted to 1:200) were suspended in ADB. The last incubation of Alexa Fluor 568 donkey anti-goat (Invitrogen; diluted 1:100) was incubated at 1:100 for 2 hours at 37°C. Slides were fixed with Prolong Gold Antifade (Invitrogen) for 24 hours after a final wash in 1x PBS. Three slides of cell spreads per mouse were prepared to serve as technical replicates for the staining protocol. Comparisons of multiple, stained slides from the same mouse showed no difference in mean MLH1 cell counts and mean cell quality. Sampled numbers of mice and cells per mouse were maximized to the extent possible given constraints on breeding and time.

## **Image Processing**

Images were captured using a Zeiss Axioplan 2 microscope with AxioLab camera and AxioVision software (Zeiss, Cambridge, UK). The number of cells imaged per individual mouse is based on previous studies (Dumont and Payseur, 2011; Murdoch et al., 2010;

Wang and Payseur, 2017). Preprocessing, including cropping, noise reduction, and histogram adjustments, was performed using Photoshop (v13.0). Image file names were anonymized before manual scoring of MLH1 foci or DMC1 foci using Photoshop.

## Analyses

To estimate the number of crossovers across the genome, we counted MLH1 foci within bivalents, synapsed homologous chromosomes. MLH1 foci were counted in pachytene cells with intact and complete karyotypes (19 acrocentric bivalents and XY for spermatocytes; 20 acrocentric bivalents for oocytes) and distinct MLH1 foci. A quality score ranging from 1 (best) to 5 (worst) was assigned to each cell based on visual appearance of staining and spread of bivalents. Cells with a score of 5 were excluded from the final analysis.

Distributions of MLH1 count per cell were visually inspected for normality (Supplemental Figure 1). When outliers for MLH1 count were found during preliminary analysis, the original images were inspected and the counts confirmed.

MLH1 foci located on the XY in spermatocytes were excluded from counts. In addition to MLH1 counts, we measured several traits to further characterize the recombination landscape. To estimate the number of double-strand breaks, a minority of which lead to crossovers, mean DMC1 foci per cell was quantified for a single male from each of a subset of strains (*molossinus*<sup>MSM</sup>, *musculus*<sup>PWD</sup>, *domesticus*<sup>WSB</sup>, and *domesticus*<sup>G</sup>). SC morphology and CREST foci number were used to stage spermatocytes as early zygotene or late zygotene.

To measure bivalent SC length, two image analysis algorithms were used. The first algorithm estimates the total (summed) SC length across bivalents for individual cells (Wang et al., 2019). The second algorithm estimates the SC length of individual bivalents (Peterson et al., 2019). Both algorithms apply a ‘skeletonizing’ transformation to synapsed chromosomes that produces a single, pixel-wide ‘trace’ of the bivalent shape. Total SC length per cell was quantified from pachytene cell images (Wang et al., 2019).

To reduce algorithmic errors in SC isolation, outliers were visually identified at the mouse level and removed from the data set. Mouse averages were calculated from cell-wide total



SC lengths in 3,195 out of 3,871 cells with MLH1 counts. SC length of individual bivalents was quantified in pachytene cell images (Peterson et al., 2019). The DNA CrossOver algorithm (Peterson et al., 2019) isolates single, straightened bivalent shapes, returning SC length, location of MLH1 foci, and location of CREST (centromere) foci. The algorithm substantially speeds the accurate measurement of bivalents, but it sometimes interprets overlapping bivalents as single bivalents. In our data set, average proportions of bivalents per cell isolated by the algorithm ranged from 0.48 (*molossinus*<sup>MSM</sup> male) to 0.72 (*musculus*<sup>KAZ</sup> female). From the total set of pachytene cell images, 10,213 bivalent objects were isolated by the algorithm. Following a manual curation, 9,569 single-bivalent observations remained. The accuracy of the algorithm is high compared to hand measures after this curation step (Peterson et al., 2019). The curated single bivalent data supplemented our cell-wide MLH1 count data with MLH1 foci counts for single bivalents. Proportions of bivalents with the same number of MLH1 foci were compared across strains using a chi-square test.

To account for confounding effects of sex chromosomes from pooled samples of bivalents, we also considered a reduced data set including only bivalents with SC lengths below the 2nd quartile in cells with at least 17 of 20 single bivalent measures. This “short bivalent” data set included the four or five shortest bivalents within a cell, thus excluding the X bivalent in oocytes. A total of 699 short bivalents were isolated from 102 oocytes and 42 spermatocytes. Although this smaller data set had decreased power, it offered a more comparable set of single bivalents to compare between the sexes. A “long bivalent” data set was formed from those bivalents above the 4th quartile in SC lengths per cell. A total of 703 long bivalents were isolated from 102 oocytes and 42 spermatocytes.

To examine crossover interference, the distance (in SC units) between MLH1 foci (inter-focal distance; IFD<sub>raw</sub>) was measured for those single bivalents containing two MLH1 foci. A normalized measure of interference (IFD<sub>norm</sub>) was computed by dividing IFD<sub>raw</sub> by SC length on a per-bivalent basis.

We used a series of statistical models to interpret patterns of variation in the recombination traits we measured (Table 2). We used mouse average as the dependent

variable in all analyses. We first constructed a linear mixed model (M1) using lmer() from the lmer4 package (Bates et al., 2015) in R (v3.5.2) (Team, 2015). In this model, strain was coded as a random effect, with significance evaluated using a likelihood ratio test using exactRLRT() from RLRsim (Scheipl et al., 2008). Subspecies, sex, and their interaction were coded as fixed effects, with significance evaluated using a chi-square test comparing the full and reduced models (drop1() and anova()) (Bates et al., 2015). The hierarchical nature of the data meant that nesting of levels across observations was implicit (*i.e.* mouse within strain, within subspecies) and not explicitly coded. We used the subspecies effect to quantify divergence between subspecies and the (random) strain effect to quantify variation within subspecies in a sex-specific manner. In separate analyses using model M1, we considered mouse averages as dependent variables for each of the following traits: MLH1 count per cell, total SC length per cell, single bivalent SC length per cell, IFD<sub>raw</sub>, IFD<sub>norm</sub>, and average MLH1 position (for single-focus bivalents). Four additional linear models containing only fixed effects (M2-M5) (Table 2) were used to further investigate results obtained from model M1.

## Acknowledgements

This research was funded by NIH grants R01GM120051 and R01GM100426 to B. A. P.. A. L. P. was partly supported by NIH T32GM007133. We are grateful to Francisco Pelegri for generous assistance with microscopy. We thank Karl Broman and Cécile Ané for advice on analyses.

## Competing interests

The authors declare that there are no competing interests.

## REFERENCES

- Anderson LK, Reeves A, Webb LM, Ashley T. 1999. Distribution of crossing over on mouse synaptonemal complexes using immunofluorescent localization of mlh1 protein. *Genetics* **151**:1569–1579.
- Baier B, Hunt P, Broman KW, Hassold T. 2014. Variation in genome-wide levels of meiotic recombination is established at the onset of prophase in mammalian males. *PLoS genetics* **10**. doi:10.1371/journal.pgen.1004125
- Bates D, Mächler M, Bolker B, Walker S. 2015. Fitting linear mixed-effects models using lme4. *Journal of Statistical Software* **67**:1–48. doi:10.18637/jss.v067.i01
- Baudat F, Imai Y, De Massy B. 2013. Meiotic recombination in mammals: Localization and regulation. *Nature Reviews Genetics* **14**:794–806. doi:10.1038/nrg3573
- Begun DJ, Aquadro CF. 1992. Levels of naturally occurring dna polymorphism correlate with recombination rates in d. *Melanogaster*. *Nature* **356**:519–520. doi:10.1038/356519a0
- Bell G. 1982. The masterpiece of nature: The evolution and genetics of sexuality. Berkeley, CA.: University of California Press.
- Bolcun-Filas E, Schimenti J. 2012. Genetics of meiosis and recombination in mice. *International review of cell and molecular biology* **298**:179. doi:https://doi.org/10.1016/B978-0-12-394309-5.00005-5
- Brandvain Y, Coop G. 2012. Scrambling eggs: Meiotic drive and the evolution of female recombination rates. *Genetics* **190**:709–723. doi:10.1534/genetics.111.136721
- Burt A, Bell G, Harvey PH. 1991. Sex differences in recombination. *Journal of evolutionary biology* **4**:259–277. doi:https://doi.org/10.1046/j.1420-9101.1991.4020259.x
- Cahoon CK, Libuda DE. 2019. Leagues of their own: Sexually dimorphic features of meiotic prophase i. *Chromosoma* 1–16. doi:10.1007/s00412-019-00692-x

503 Charlesworth B, Morgan M, Charlesworth D. 1993. The effect of deleterious mutations on  
504 neutral molecular variation. *Genetics* **134**:1289–1303.

505 Cutter AD, Payseur BA. 2013. Genomic signatures of selection at linked sites: Unifying the  
506 disparity among species. *Nature Reviews Genetics* **14**:262–274.  
507 doi:<https://doi.org/10.1038/nrg3425>

508 Dapper AL, Payseur BA. 2017. Connecting theory and data to understand recombination  
509 rate evolution. *Philosophical Transactions of the Royal Society B: Biological Sciences*  
510 **372**:20160469. doi:10.1098/rstb.2016.0469

511 Dumont BL, Payseur BA. 2011. Evolution of the genomic recombination rate in murid  
512 rodents. *Genetics* **187**:643–657. doi:10.1534/genetics.110.123851

513 Dumont J, Desai A. 2012. Acentrosomal spindle assembly and chromosome segregation  
514 during oocyte meiosis. *Trends in cell biology* **22**:241–249. doi:10.1016/j.tcb.2012.02.007

515 Felsenstein J. 1974. The evolutionary advantage of recombination. *Genetics* **78**:737–756.

516 Fisher RA. 1930. The genetical theory of natural selection. Oxford University Press.

517 Fledel-Alon A, Leffler EM, Guan Y, Stephens M, Coop G, Przeworski M. 2011. Variation in  
518 human recombination rates and its genetic determinants. *PloS one* **6**.  
519 doi:10.1371/journal.pone.0020321

520 Geraldès A, Basset P, Smith KL, Nachman MW. 2011. Higher differentiation among  
521 subspecies of the house mouse (*mus musculus*) in genomic regions with low  
522 recombination. *Molecular ecology* **20**:4722–4736. doi:10.1111/j.1365-294X.2011.05285.x

523 Goldstein DB, Bergman A, Feldman MW. 1993. The evolution of interference: Reduction of  
524 recombination among three loci. *Theoretical population biology* **44**:246–259.  
525 doi:10.1006/tpbi.1993.1028

526 Gruhn JR, Rubio C, Broman KW, Hunt PA, Hassold T. 2013. Cytological studies of human  
527 meiosis: Sex-specific differences in recombination originate at, or prior to, establishment of  
528 double-strand breaks. *PloS one* **8**. doi:10.1371/journal.pone.0085075

529 Haenel Q, Laurentino TG, Roesti M, Berner D. 2018. Meta-analysis of chromosome-scale  
530 crossover rate variation in eukaryotes and its significance to evolutionary genomics.  
531 *Molecular ecology* **27**:2477–2497. doi:10.1111/mec.14699

532 Haldane J. 1922. Sex ratio and unisexual sterility in hybrid animals. *Journal of genetics*  
533 **12**:101–109.

534 Halldorsson BV, Palsson G, Stefansson OA, Jonsson H, Hardarson MT, Eggertsson HP,  
535 Gunnarsson B, Oddsson A, Halldorsson GH, Zink F, others. 2019. Characterizing mutagenic  
536 effects of recombination through a sequence-level genetic map. *Science* **363**:eaau1043.  
537 doi:10.1126/science.aau1043

538 Handel MA, Schimenti JC. 2010. Genetics of mammalian meiosis: Regulation, dynamics and  
539 impact on fertility. *Nature Reviews Genetics* **11**:124–136. doi:10.1038/nrg2723

540 Hassold T, Hunt P. 2001. To err (meiotically) is human: The genesis of human aneuploidy.  
541 *Nature Reviews Genetics* **2**:280–291. doi:https://doi.org/10.1038/35066065

542 Hill WG, Robertson A. 1966. The effect of linkage on limits to artificial selection. *Genetics*  
543 *Research* **8**:269–294. doi:https://doi.org/10.1017/S0016672300010156

544 Holloway JK, Booth J, Edelmann W, McGowan CH, Cohen PE. 2008. MUS81 generates a  
545 subset of mlh1–mlh3–independent crossovers in mammalian meiosis. *PLoS genetics* **4**.  
546 doi:10.1371/journal.pgen.1000186

547 Hultén MA. 2011. On the origin of crossover interference: A chromosome oscillatory  
548 movement (com) model. *Molecular cytogenetics* **4**:10. doi:10.1186/1755-8166-4-10

549 Huxley J. 1928. Sexual difference of linkage in *gammarus chevreuxi*. *Journal of Genetics*  
550 **20**:145–156.

551 Inoue K, Lupski JR. 2002. Molecular mechanisms for genomic disorders. *Annual review of*  
552 *genomics and human genetics* **3**:199–242. doi:10.1146/annurev.genom.3.032802.120023

553 Johnston SE, Bérénos C, Slate J, Pemberton JM. 2016. Conserved genetic architecture  
 554 underlying individual recombination rate variation in a wild population of soay sheep (*ovis*  
 555 *aries*). *Genetics* **203**:583–598. doi:10.1534/genetics.115.185553

556 Koehler KE, Cherry JP, Lynn A, Hunt PA, Hassold TJ. 2002. Genetic control of mammalian  
 557 meiotic recombination. I. Variation in exchange frequencies among males from inbred  
 558 mouse strains. *Genetics* **162**:297–306.

559 Kong A, Barnard J, Gudbjartsson DF, Thorleifsson G, Jonsdottir G, Sigurdardottir S,  
 560 Richardsson B, Jonsdottir J, Thorgeirsson T, Frigge ML, others. 2004. Recombination rate  
 561 and reproductive success in humans. *Nature genetics* **36**:1203–1206. doi:10.1038/ng1445

562 Kong A, Thorleifsson G, Frigge ML, Masson G, Gudbjartsson DF, Villemoes R, Magnusdottir  
 563 E, Olafsdottir SB, Thorsteinsdottir U, Stefansson K. 2014. Common and low-frequency  
 564 variants associated with genome-wide recombination rate. *Nature genetics* **46**:11.  
 565 doi:10.1038/ng.2833

566 Kong A, Thorleifsson G, Stefansson H, Masson G, Helgason A, Gudbjartsson DF, Jonsdottir  
 567 GM, Gudjonsson SA, Sverrisson S, Thorlacius T, others. 2008. Sequence variants in the  
 568 *rnf212* gene associate with genome-wide recombination rate. *Science* **319**:1398–1401.  
 569 doi:10.1126/science.1152422

570 Kudo NR, Anger M, Peters AH, Stemmann O, Theussl H-C, Helmhart W, Kudo H, Heyting C,  
 571 Nasmyth K. 2009. Role of cleavage by separase of the *rec8* kleisin subunit of cohesin during  
 572 mammalian meiosis i. *Journal of cell science* **122**:2686–2698. doi:10.1242/jcs.035287

573 Kyogoku H, Kitajima TS. 2017. Large cytoplasm is linked to the error-prone nature of  
 574 oocytes. *Developmental cell* **41**:287–298. doi:10.1016/j.devcel.2017.04.009

575 Lane S, Kauppi L. 2019. Meiotic spindle assembly checkpoint and aneuploidy in males  
 576 versus females. *Cellular and molecular life sciences* **76**:1135–1150. doi:10.1007/s00018-  
 577 018-2986-6

578 Lee J. 2019. Is age-related increase of chromosome segregation errors in mammalian  
 579 oocytes caused by cohesin deterioration? *Reproductive Medicine and Biology*.  
 580 doi:10.1002/rmb2.12299

581 Lenormand T. 2003. The evolution of sex dimorphism in recombination. *Genetics* **163**:811–  
 582 822.

583 Lenormand T, Dutheil J. 2005. Recombination difference between sexes: A role for haploid  
 584 selection. *PLoS biology* **3**. doi:10.1371/journal.pbio.0030063

585 Lenormand T, Engelstädter J, Johnston SE, Wijnker E, Haag CR. 2016. Evolutionary  
 586 mysteries in meiosis. *Philosophical Transactions of the Royal Society B: Biological Sciences*  
 587 **371**:20160001. doi:10.1098/rstb.2016.0001

588 Lorch P. 2005. Sex differences in recombination and mapping adaptations. *Genetica* **123**:39.  
 589 doi:10.1007/s10709-003-2706-4

590 Lynn A, Koehler KE, Judis L, Chan ER, Cherry JP, Schwartz S, Seftel A, Hunt PA, Hassold TJ.  
 591 2002. Covariation of synaptonemal complex length and mammalian meiotic exchange rates.  
 592 *Science* **296**:2222–2225.

593 Ma L, O’Connell JR, VanRaden PM, Shen B, Padhi A, Sun C, Bickhart DM, Cole JB, Null DJ, Liu  
 594 GE, others. 2015. Cattle sex-specific recombination and genetic control from a large  
 595 pedigree analysis. *PLoS genetics* **11**. doi:10.1371/journal.pgen.1005387

596 Murdoch B, Owen N, Shirley S, Crumb S, Broman KW, Hassold T. 2010. Multiple loci  
 597 contribute to genome-wide recombination levels in male mice. *Mammalian Genome*  
 598 **21**:550–555. doi:https://doi.org/10.1007/s00335-010-9303-5

599 Nachman MW, Payseur BA. 2012. Recombination rate variation and speciation: Theoretical  
 600 predictions and empirical results from rabbits and mice. *Philosophical Transactions of the*  
 601 *Royal Society B: Biological Sciences* **367**:409–421. doi:10.1098/rstb.2011.0249

602 Nagaoka SI, Hassold TJ, Hunt PA. 2012. Human aneuploidy: Mechanisms and new insights  
 603 into an age-old problem. *Nature Reviews Genetics* **13**:493–504. doi:10.1038/nrg3245

604 Otto SP, Payseur BA. 2019. Crossover interference: Shedding light on the evolution of  
 605 recombination. *Annual review of genetics* **53**:19–44. doi:10.1146/annurev-genet-040119-  
 606 093957

607 Peters AH, Plug AW, Vugt MJ van, De Boer P. 1997. SHORT COMMUNICATIONS A drying-  
 608 down technique for the spreading of mammalian meiocytes from the male and female  
 609 germline. *Chromosome research* **5**:66–68. doi:10.1023/A:1018445520117

610 Peterson AL, Miller ND, Payseur BA. 2019. Conservation of the genome-wide recombination  
 611 rate in white-footed mice. *Heredity* **123**:442–457. doi:10.1038/s41437-019-0252-9

612 Petkov PM, Broman KW, Szatkiewicz JP, Paigen K. 2007. Crossover interference underlies  
 613 sex differences in recombination rates. *Trends in Genetics* **23**:539–542.  
 614 doi:10.1016/j.tig.2007.08.015

615 Petronczki M, Siomos MF, Nasmyth K. 2003. Un menage a quatre: The molecular biology of  
 616 chromosome segregation in meiosis. *Cell* **112**:423–440.  
 617 doi:https://doi.org/10.1016/S0092-8674(03)00083-7

618 Ritz KR, Noor MA, Singh ND. 2017. Variation in recombination rate: Adaptive or not? *Trends*  
 619 *in Genetics* **33**:364–374. doi:10.1016/j.tig.2017.03.003

620 Samuk K, Manzano-Winkler B, Ritz KR, Noor MA. 2020. Natural selection shapes variation  
 621 in genome-wide recombination rate in drosophila pseudoobscura. *Current Biology*.  
 622 doi:10.1016/j.cub.2020.03.053

623 Sardell JM, Kirkpatrick M. 2020. Sex differences in the recombination landscape. *The*  
 624 *American Naturalist* **195**:361–379. doi:10.1086/704943

625 Scheipl F, Greven S, Kuechenhoff H. 2008. Size and power of tests for a zero random effect  
 626 variance or polynomial regression in additive and linear mixed models. *Computational*  
 627 *Statistics & Data Analysis* **52**:3283–3299. doi:10.1016/j.csda.2007.10.022

628 Segura J, Ferretti L, Ramos-Onsins S, Capilla L, Farré M, Reis F, Oliver-Bonet M, Fernández-  
 629 Bellón H, Garcia F, Garcia-Caldés M, others. 2013. Evolution of recombination in eutherian



630 mammals: Insights into mechanisms that affect recombination rates and crossover  
631 interference. *Proceedings of the Royal Society B: Biological Sciences* **280**:20131945.  
632 doi:10.1098/rspb.2013.1945

633 Shen B, Jiang J, Seroussi E, Liu GE, Ma L. 2018. Characterization of recombination features  
634 and the genetic basis in multiple cattle breeds. *BMC genomics* **19**:304. doi:10.1186/s12864-  
635 018-4705-y

636 Smith JM, Haigh J. 1974. The hitch-hiking effect of a favourable gene. *Genetics Research*  
637 **23**:23–35. doi:https://doi.org/10.1017/S0016672300014634

638 So C, Seres KB, Steyer AM, Mönnich E, Clift D, Pejkovska A, Möbius W, Schuh M. 2019. A  
639 liquid-like spindle domain promotes acentrosomal spindle assembly in mammalian  
640 oocytes. *Science* **364**:eaat9557. doi:10.1126/science.aat9557

641 Subramanian VV, Hochwagen A. 2014. The meiotic checkpoint network: Step-by-step  
642 through meiotic prophase. *Cold Spring Harbor perspectives in biology* **6**:a016675.  
643 doi:10.1101/cshperspect.a016675

644 Team R. 2015. RStudio: Integrated Development Environment for R.

645 Tease C, Hulten M. 2004. Inter-sex variation in synaptonemal complex lengths largely  
646 determine the different recombination rates in male and female germ cells. *Cytogenetic and*  
647 *genome research* **107**:208–215. doi:10.1159/000080599

648 VanVeen JE, Hawley RS. 2003. Meiosis: When even two is a crowd. *Current Biology*  
649 **13**:R831–R833. doi:10.1016/j.cub.2003.12.004

650 Wang RJ, Dumont BL, Jing P, Payseur BA. 2019. A first genetic portrait of synaptonemal  
651 complex variation. *PLoS genetics* **15**:e1008337. doi:10.1371/journal.pgen.1008337

652 Wang RJ, Payseur BA. 2017. Genetics of genome-wide recombination rate evolution in mice  
653 from an isolated island. *Genetics* **206**:1841–1852. doi:10.1534/genetics.117.202382

654 Wang S, Hassold T, Hunt P, White MA, Zickler D, Kleckner N, Zhang L. 2017. Inefficient  
655 crossover maturation underlies elevated aneuploidy in human female meiosis. *Cell*  
656 **168**:977–989. doi:10.1016/j.cell.2017.02.002

657 Wong AK, Ruhe AL, Dumont BL, Robertson KR, Guerrero G, Shull SM, Ziegler JS, Millon LV,  
658 Broman KW, Payseur BA, others. 2010. A comprehensive linkage map of the dog genome.  
659 *Genetics* **184**:595–605. doi:10.1534/genetics.109.106831

660

661

Figures

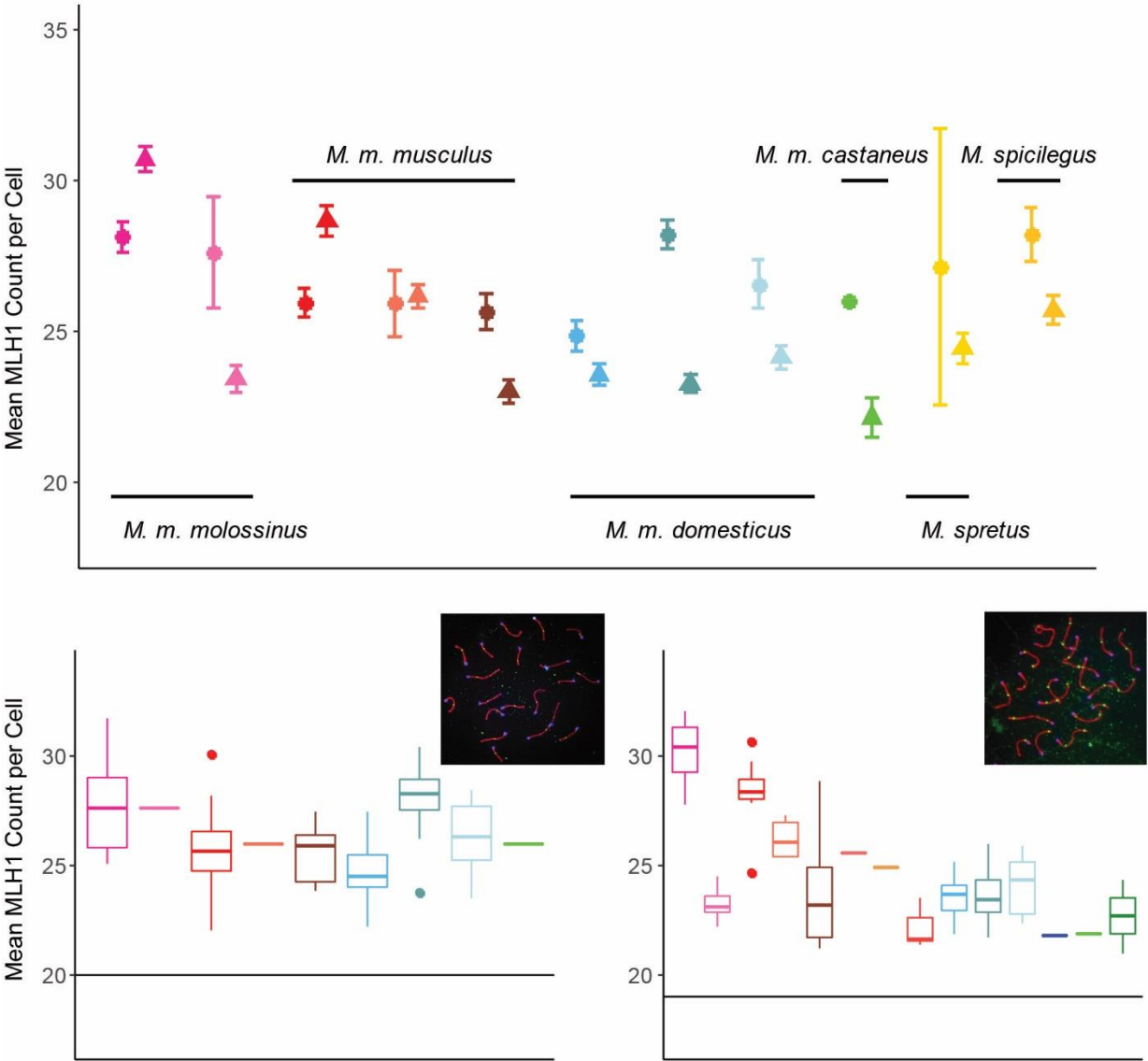


Figure 1. MLH1 Counts. A) Strain mean MLH1 counts (+/- 2 standard errors) in both sexes. Females = circles; males = triangles. B) Boxplots of female MLH1 counts for strains of house mice. Whiskers indicate interquartile range. Inset: example oocyte, SYCP3 stained in red, CREST (centromeres) stained in blue and MLH1 foci stained in green. Horizontal line at 20 indicates the expected minimum number of foci per cell. C) Boxplots of male MLH1 counts for strains of house mice. Inset: example spermatocyte. Additional strains with only male observations are included with the values from Table 2.

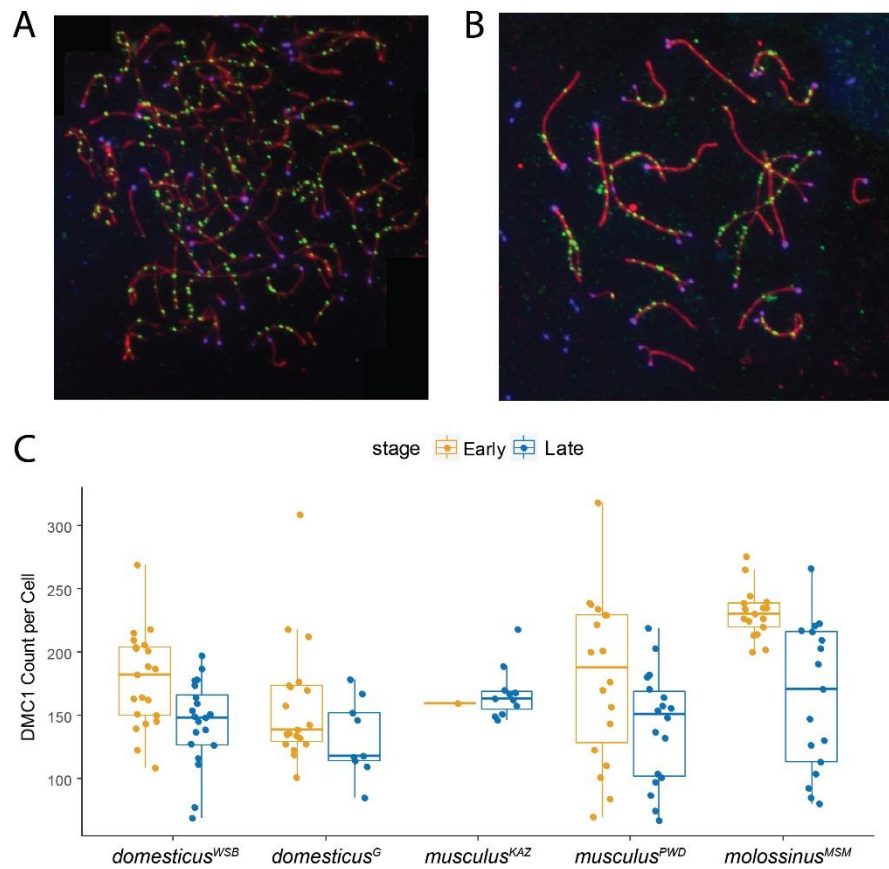


Figure 2. DMC1 Counts in Males. A) Example early zygotene spermatocyte spread. SYCP3 stained in red, CREST (centromeres) stained in blue and DMC1 stained in green. B) Example late zygotene spermatocyte spread. C) Boxplots of DMC1 counts for strains of house mice. Whiskers indicate interquartile range.

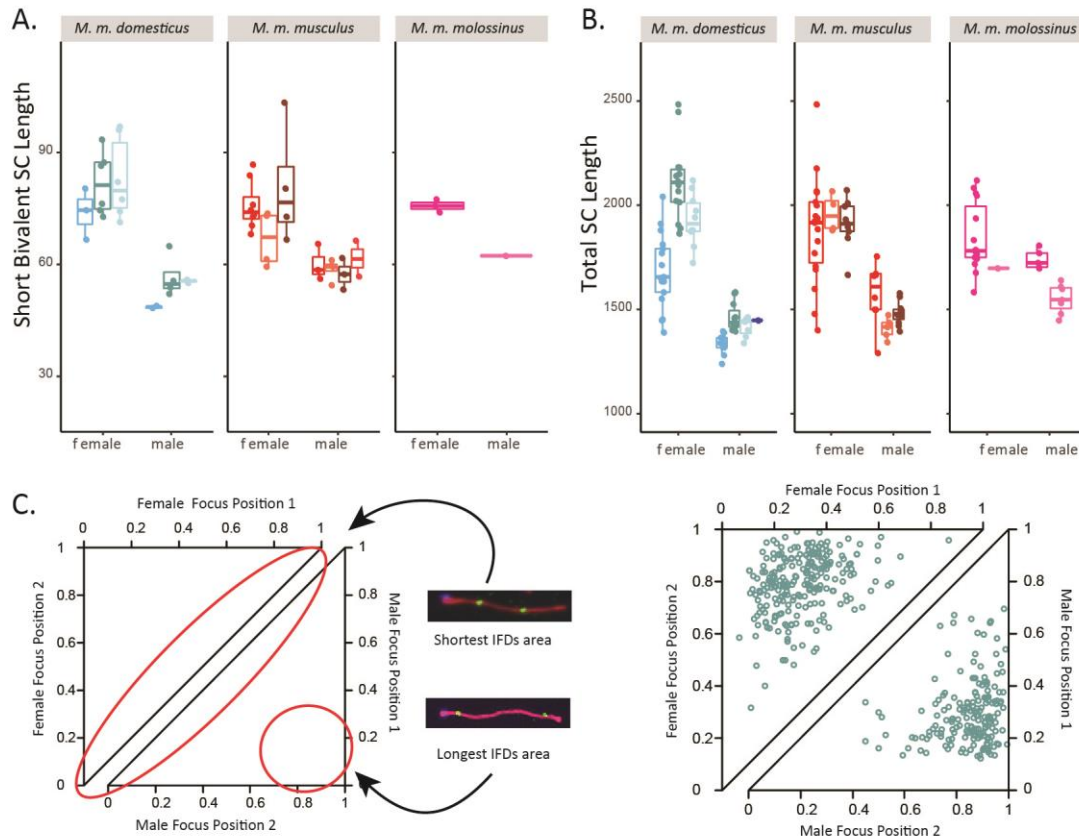


Figure 3. Sex Differences in Synaptonemal Complex (SC) Length and MLH1 Foci Positions. A) Mouse average SC length of short bivalents. Whiskers indicate interquartile range. B) Mouse average total SC length. C) Example of sex differences in inter-focal distances and foci locations on bivalents with two foci. Female observations shown in top triangle; male observations shown in bottom triangle. Data from *domesticus*<sup>G</sup>.

## Tables

Table 1

Species	Subspecies	Strain	Sex	Number of Mice	Number of Cells	Mean MLH1 Count	SE	cV	Variance
<i>M. musculus</i>	<i>M. m. domesticus</i>	WSB	female	14	184	24.70	0.27	14.64	13.07
			male	11	222	23.38	0.18	11.48	7.21
		G	female	12	318	28.21	0.24	14.84	17.52
			male	18	355	23.16	0.14	11.35	6.92
		LEW	female	9	147	26.59	0.40	18.16	23.31
			male	10	253	24.16	0.20	12.84	9.62
		PERC	male	1	26	21.81	0.41	9.71	4.48
	<i>M. m. musculus</i>	PWD	female	15	222	25.98	0.25	14.41	14.01
			male	8	161	28.67	0.25	10.90	9.76
		SKIVE	female	1	32	25.94	0.55	12.07	9.80
			male	3	86	26.08	0.29	10.41	7.37
		KAZ	female	9	184	25.63	0.30	15.63	16.04
			male	13	264	22.99	0.19	13.16	9.15
		CZECH	male	3	62	22.30	0.32	11.21	6.25
		AST	male	3	63	24.41	0.33	10.65	6.76
		TOM	male	2	10	23.70	1.18	15.79	14.01
	<i>M. m. castaneus</i>	CAST	female	1	1	26.00	NA	NA	NA
			male	2	44	22.00	0.34	10.00	5.20
		HMI	male	4	44	24.00	0.41	11.00	7.50
	<i>M. m. molossinus</i>	MSM	female	14	300	28.12	0.25	15.64	19.35
			male	7	166	30.37	0.24	10.26	9.71
		MOLF	female	1	21	27.62	0.92	15.34	17.95
			male	6	119	23.42	0.23	10.80	6.40
<i>Mus spretus</i>		SPRET	female	2	2	26.00	2.00	10.88	8.00
			male	5	103	24.43	0.25	10.23	6.25
<i>Mus spicilegus</i>		SPIC	female	6	97	28.24	0.45	15.63	19.47
			male	4	133	25.77	0.24	10.78	7.72
<i>Mus caroli</i>		CAROLI	male	2	57	27.00	0.40	11.00	8.90

Table 2

Model	Dataset(s)	Dependent Variable(s)	Fixed Effects	Random Effects
M1	females and males from 8 strains	mouse average	subspecies sex subspecies*sex	strain
M2	females and males from 8 strains	mouse average	subspecies sex strain subspecies*sex subspecies*strain sex*strain	
M3	females and males from 8 strains	mouse average	sex strain sex*strain	
M4	females from 8 strains	female mouse average	subspecies  strain subspecies*strain	
M4	males from 12 strains	male mouse average	subspecies  strain subspecies*strain	
M5	females from 8 strains	female mouse average	strain	
M5	males from 12 strains	male mouse average	strain	

Table 3

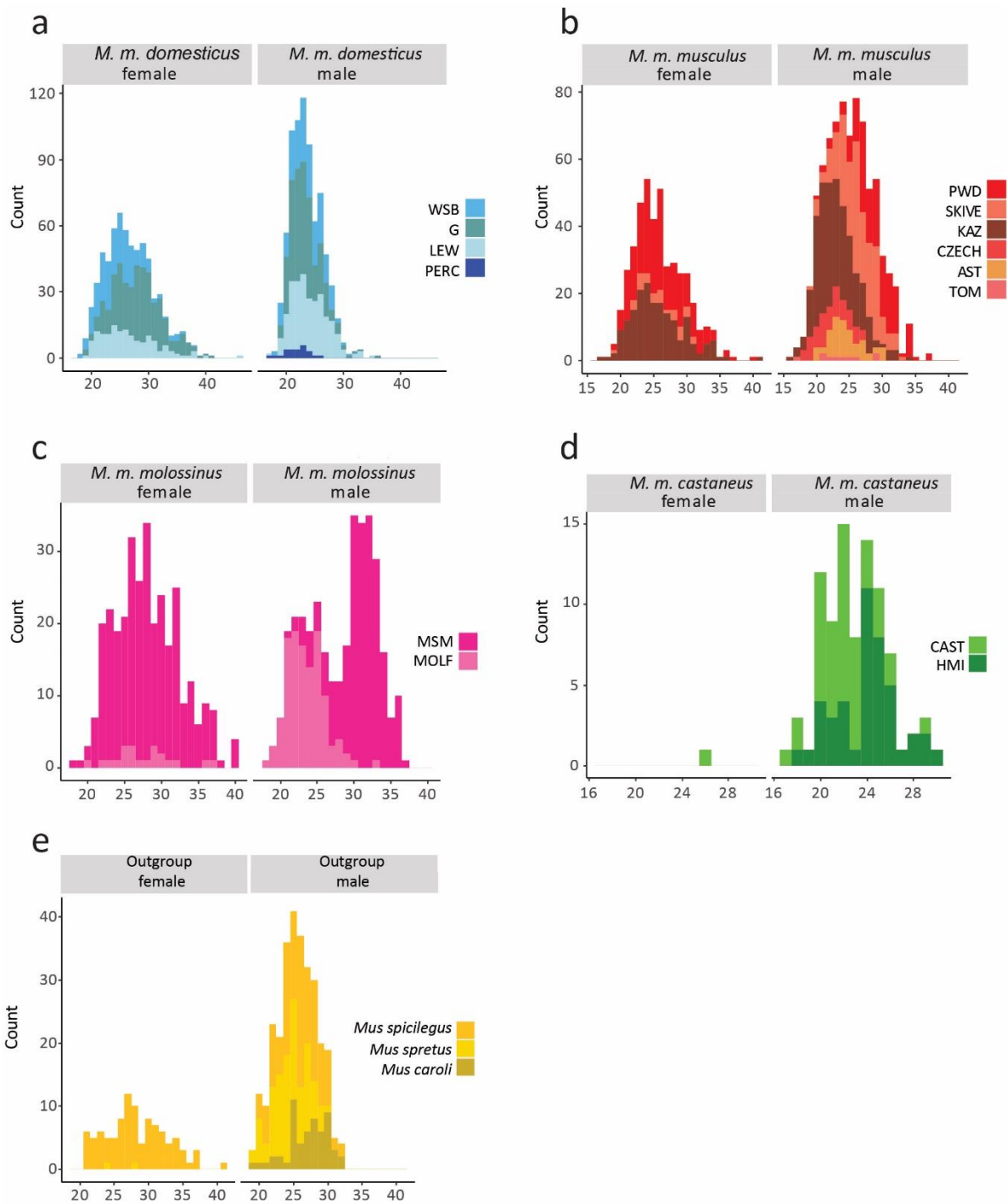
Recombination Group	Strain	Early Zygotene			Late Zygotene		
		Cells	Mean	MLH1:DMC1 Ratio	Cells	Mean	MLH1:DMC1 Ratio
Low	<i>domesticus</i> <sup>WSB</sup>	21	177.76	0.14	20	144.25	0.17
	<i>domesticus</i> <sup>G</sup>	19	158.16	0.15	9	131.78	0.18
	<i>musculus</i> <sup>KAZ</sup>	1	159.00	0.15	11	167.36	0.14
High	<i>musculus</i> <sup>PWD</sup>	18	180.22	0.16	18	140.78	0.21
	<i>molossinus</i> <sup>MSM</sup>	17	231.00	0.14	17	164.41	0.19

Table 4

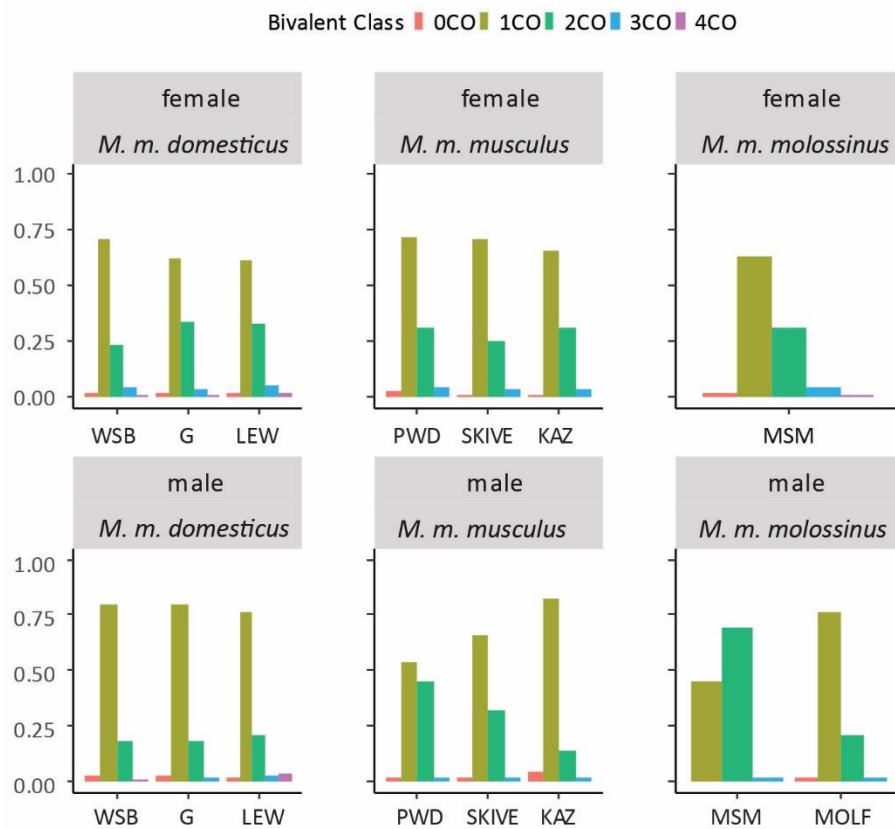
Species	Strain Name	Abbreviation	Geographic Origin	Source
<i>M. m. domesticus</i>		G	Gough Island	Payseur Laboratory
	LEWES/EiJ	LEW	Lewes, Delaware	Jackson Laboratory
	PERC/EiJ	PERC	Peru	Jackson Laboratory
	WSB/EiJ	WSB	Eastern Shore, Maryland	Jackson Laboratory
<i>M. m. musculus</i>	AST/TUA	AST	Astrakhan, Russia	BRC RIKEN
	CZECHII/EiJ	CZECH	Slovakia	Jackson Laboratory
	KAZ/TUA	KAZ	Alma-Ata, Kazakhstan	BRC RIKEN
	PWD/PhJ	PWD	Prague, Czech Republic	Jackson Laboratory
	SKIVE/EiJ	SKIVE	Skive, Denmark	Jackson Laboratory
	TOM/TUA	TOM	Tomsk, Russia	BRC RIKEN
<i>M. m. molossinus</i>	MOLF/EiJ	MOLF	Kyushu, Japan	Jackson Laboratory
	MSM/MsJ	MSM	Mishima, Japan	Jackson Laboratory
<i>M. m. castaneus</i>	CAST/EiJ	CAST	Thailand	Jackson Laboratory
	HMI/Ms	HMI	Hemei, Taiwan	BRC RIKEN
<i>Mus spertus</i>	SPRET/EiJ	SPRET	Cadiz, Spain	Jackson Laboratory
<i>Mus spicilegus</i>	SPI/TUA	SPI	Mt. Caocacus, Bulgaria	BRC RIKEN
<i>Mus caroli</i>	CAR	CAROLI	Thailand	BRC RIKEN



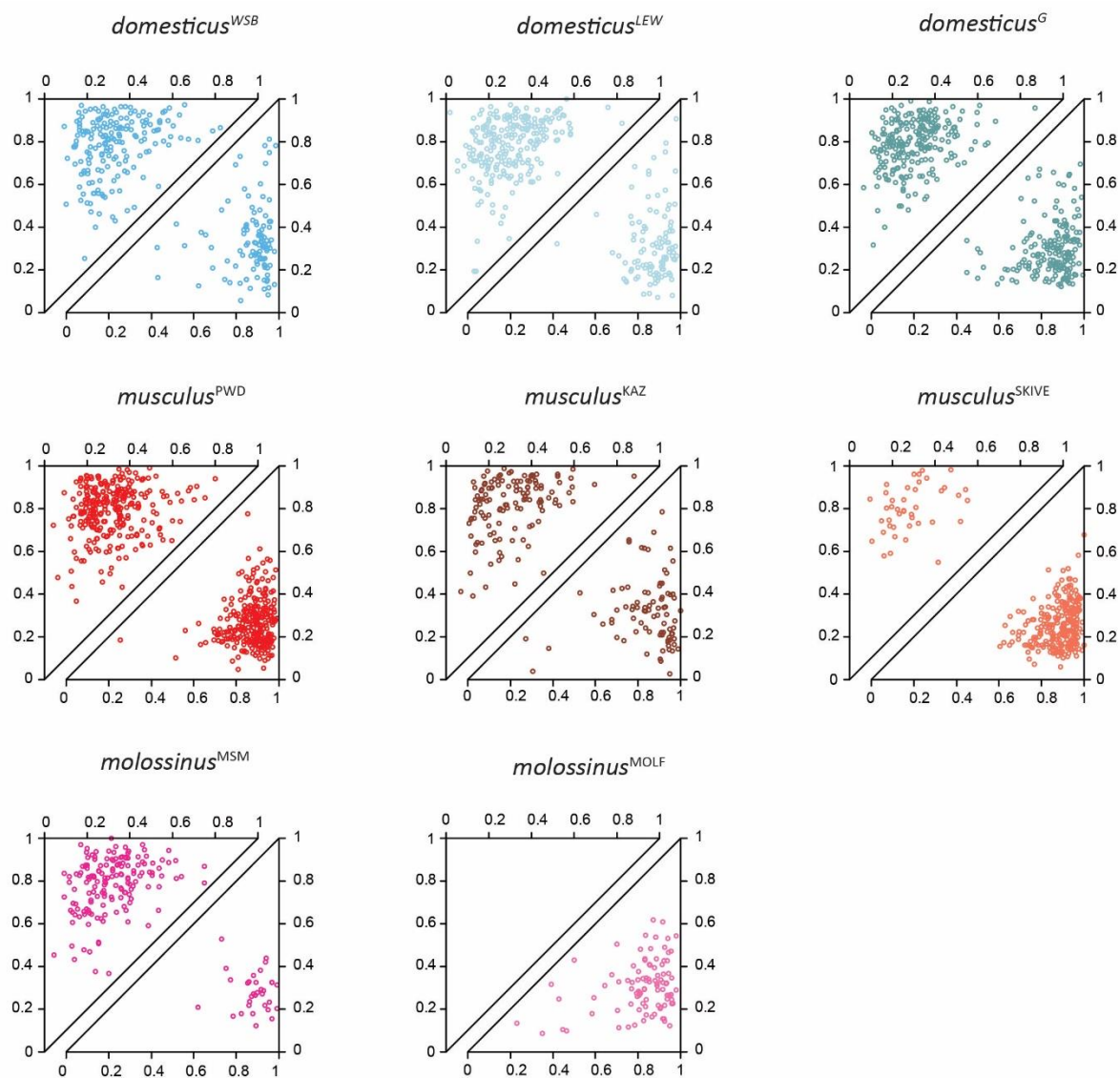
Supplemental Figures



Supplemental Figure 1 Distributions of MLH1 Counts per Cell. Strain names are abbreviated for space.



*Supplemental Figure 2. Proportions of Bivalents with Different Numbers of MLH1 Foci. Strain names are abbreviated for space.*



*Supplemental Figure 3. Inter-focal Distances on Bivalents with Two MLH1 Foci. Each point shows the positions of both foci, normalized by bivalent SC length. Observations are separated by sex (females=top triangles; males=bottom triangles).*

## Supplemental Tables

*Supplemental Table 1*

<b>M1 MLH1 Count</b>	<b>p values</b>		<b>Coefficients (fixed estimates)</b>	<b>Random Effects (standard deviation)</b>
Subspecies	0.00097	Intercept	26.356	
Sex	0.00000	Subspecies Musculus	-0.755	
Subspecies*Sex	0.00018	Subspecies Molossinus	-0.482	
strain(random)	0.00010	Sex(male)	-2.649	
		Musculus*male	2.953	
		Molossinus*male	3.201	
		intercept		1.69
		Strain		1.89

*Supplemental Table 2*

<b>M2 MLH1 Count</b>	<b>Estimate</b>	<b>Std. Error</b>	<b>t value</b>	<b>Pr(&gt; t )</b>
(Intercept)	24.718	0.447	55.356	0.000
Subspecies Musculus	0.849	0.714	1.190	0.236
Subspecies Molossinus	2.901	1.729	1.678	0.096
Sex (male)	-1.194	0.692	-1.726	0.087
Strain G	3.301	0.657	5.023	0.000
Strain LEW	1.694	0.714	2.373	0.019
Strain PWD	0.257	0.704	0.365	0.716
Strain MSM	0.086	1.729	0.050	0.960
Strain SKIVE	0.371	1.761	0.210	0.834
Subspecies Musculus * Sex	-0.768	1.021	-0.753	0.453
Subspecies Molossinus * Sex	-3.185	1.933	-1.648	0.102
Strain G * Sex (male)	-3.144	0.982	-3.201	0.002
Strain LEW * Sex (male)	-1.165	1.090	-1.070	0.287
Strain PWD * Sex (male)	4.444	1.048	4.239	0.000
Strain MSM * Sex (male)	6.826	2.038	3.349	0.001
Strain SKIVE * Sex (male)	2.260	1.978	1.143	0.255

*Supplemental Table 3*

<b>M3 MLH1 Count</b>	<b>Estimate</b>	<b>Std. Error</b>	<b>t value</b>	<b>Pr(&gt; t )</b>
(Intercept)	24.718	0.447	55.356	0.000
Sex (male)	-1.194	0.692	-1.726	0.087
Strain G	3.301	0.657	5.023	0.000
Strain LEW	1.694	0.714	2.373	0.019
Strain PWD	1.107	0.621	1.783	0.077
Strain MSM	2.988	0.631	4.731	0.000
Strain MOLF	2.901	1.729	1.678	0.096
Strain SKIVE	1.220	1.729	0.706	0.482
Strain KAZ	0.849	0.714	1.190	0.236
Strain G * Sex (male)	-3.144	0.982	-3.201	0.002
Strain LEW * Sex (male)	-1.165	1.090	-1.070	0.287
Strain PWD * Sex (male)	3.675	1.007	3.651	0.000
Strain MSM * Sex (male)	3.641	1.173	3.104	0.002
Strain MOLF * Sex (male)	-3.185	1.933	-1.648	0.102
Strain SKIVE * Sex (male)	1.492	1.957	0.762	0.447
Strain KAZ * Sex (male)	-0.768	1.021	-0.753	0.453

*Supplemental Table 4*

<b>M4 Female MLH1 Count</b>	<b>Estimate</b>	<b>Std. Error</b>	<b>t value</b>	<b>Pr(&gt; t )</b>
(Intercept)	24.718	0.466	53.088	0.000
Subspecies Musculus	0.849	0.744	1.141	0.258
Subspecies Molossinus	2.901	1.803	1.609	0.112
Strain G	3.301	0.685	4.817	0.000
Strain LEW	1.694	0.744	2.276	0.026
Strain PWD	0.257	0.735	0.350	0.727
Strain MSM	0.086	1.803	0.048	0.962
Strain SKIVE	0.371	1.836	0.202	0.841

*Supplemental Table 5*

<b>M5 Female MLH1 Count</b>	<b>Estimate</b>	<b>Std. Error</b>	<b>t value</b>	<b>Pr(&gt; t )</b>
(Intercept)	24.718	0.466	53.088	0.000
Strain G	3.301	0.685	4.817	0.000
Strain LEW	1.694	0.744	2.276	0.026
Strain PWD	1.107	0.647	1.710	0.092
Strain MSM	2.988	0.658	4.537	0.000
Strain MOLF	2.901	1.803	1.609	0.112
Strain SKIVE	1.220	1.803	0.677	0.501
Strain KAZ	0.849	0.744	1.141	0.258

*Supplemental Table 6*

<b>M4 Male MLH1 Count</b>	<b>Estimate</b>	<b>Std. Error</b>	<b>t value</b>	<b>Pr(&gt; t )</b>
(Intercept)	23.524	0.495	47.530	0.000
Subspecies Musculus	-1.330	1.030	-1.291	0.202
Subspecies Molossinus	-0.284	0.808	-0.352	0.727
Strain G	0.157	0.684	0.229	0.820
Strain LEW	0.528	0.771	0.685	0.496
Strain PERC	-1.716	1.641	-1.045	0.300
Strain PWD	6.113	1.060	5.769	0.000
Strain MSM	6.913	1.010	6.843	0.000
Strain SKIVE	4.042	1.143	3.537	0.001
Strain KAZ	1.411	1.019	1.385	0.172
Strain TOM	3.406	1.807	1.885	0.065
Strain AST	2.703	1.807	1.496	0.140

*Supplemental Table 7*

<b>M5 Male MLH1 Count</b>	<b>Estimate</b>	<b>Std. Error</b>	<b>t value</b>	<b>Pr(&gt; t )</b>
(Intercept)	23.524	0.495	47.530	0.000
Strain G	0.157	0.684	0.229	0.820
Strain LEW	0.528	0.771	0.685	0.496
Strain PERC	-1.716	1.641	-1.045	0.300
Strain PWD	4.782	0.742	6.442	0.000
Strain MSM	6.629	0.926	7.159	0.000
Strain MOLF	-0.284	0.808	-0.352	0.727
Strain SKIVE	2.712	0.857	3.164	0.003
Strain KAZ	0.081	0.684	0.118	0.906
Strain TOM	2.076	1.641	1.265	0.211
Strain AST	1.373	1.641	0.836	0.406
Strain CZECH	-1.330	1.030	-1.291	0.202

*Supplemental Table 8*

<b>M1 Total SC Length</b>	<b>p values</b>		<b>Coefficients (fixed estimates)</b>	<b>Random Effects (standard deviation)</b>
Subspecies	0.00085	Intercept	1960.2	
Sex	0.00000	Subspecies Musculus	-44.1	
Subspecies*Sex	0.00010	Subspecies Molossinus	-119.1	
Strain(random)	0.00010	Sex(male)	-558	
		Musculus*male	167.1	
		Molossinus*male	396.9	
		Intercept		119
		Strain		263

*Supplemental Table 9*

<b>M2 Total SC Length</b>	<b>Estimate</b>	<b>Std. Error</b>	<b>t value</b>	<b>Pr(&gt; t )</b>
(Intercept)	1683.383	36.479	46.147	0.000
Subspecies Musculus	229.568	62.002	3.703	0.000
Subspecies Molossinus	161.137	53.281	3.024	0.003
Strain G	431.238	54.282	7.944	0.000
Strain LEW	248.684	59.941	4.149	0.000
Strain PWD	-26.764	61.403	-0.436	0.664
Strain SKIVE	50.076	90.383	0.554	0.580
Sex (male)	-345.005	58.200	-5.928	0.000
Subspecies Musculus * Sex (male)	-84.338	89.204	-0.945	0.346
Subspecies Molossinus * Sex (male)	243.125	97.055	2.505	0.013
Strain G * Sex (male)	-303.270	84.021	-3.609	0.000
Strain LEW * Sex (male)	-169.848	94.240	-1.802	0.074
Strain PWD * Sex (male)	121.505	93.030	1.306	0.194
Strain SKIVE * Sex (male)	-119.766	121.449	-0.986	0.326

*Supplemental Table 10*

<b>M3 Total SC Length</b>	<b>Estimate</b>	<b>Std. Error</b>	<b>t value</b>	<b>Pr(&gt; t )</b>
(Intercept)	1683.383	36.479	46.147	0.000
Strain G	431.238	54.282	7.944	0.000
Strain LEW	248.684	59.941	4.149	0.000
Strain PWD	202.805	50.867	3.987	0.000
Strain MSM	161.137	53.281	3.024	0.003
Strain SKIVE	279.644	83.583	3.346	0.001
Strain KAZ	229.568	62.002	3.703	0.000
Sex (male)	-345.005	58.200	-5.928	0.000
Strain G * Sex (male)	-303.270	84.021	-3.609	0.000
Strain LEW * Sex (male)	-169.848	94.240	-1.802	0.074
Strain PWD * Sex (male)	37.168	86.439	0.430	0.668
Strain MSM * Sex (male)	243.125	97.055	2.505	0.013
Strain SKIVE * Sex (male)	-204.104	116.478	-1.752	0.082
Strain KAZ * Sex (male)	-84.338	89.204	-0.945	0.346



*Supplemental Table 11*

<b>M4 Female Total SC Length</b>	<b>Estimate</b>	<b>Std. Error</b>	<b>t value</b>	<b>Pr(&gt; t )</b>
(Intercept)	1683.383	44.414	37.902	0.000
Subspecies Musculus	229.568	75.489	3.041	0.003
Subspecies Molossinus	15.823	188.432	0.084	0.933
Strain G	431.238	66.090	6.525	0.000
Strain LEW	248.684	72.979	3.408	0.001
Strain PWD	-26.764	74.760	-0.358	0.721
Strain MSM	145.314	189.128	0.768	0.445
Strain SKIVE	50.076	110.043	0.455	0.650

*Supplemental Table 12*

<b>M5 Female Total SC Length</b>	<b>Estimate</b>	<b>Std. Error</b>	<b>t value</b>	<b>Pr(&gt; t )</b>
(Intercept)	1683.383	44.414	37.902	0.000
Strain G	431.238	66.090	6.525	0.000
Strain LEW	248.684	72.979	3.408	0.001
Strain PWD	202.805	61.932	3.275	0.002
Strain MSM	161.137	64.870	2.484	0.015
Strain MOLF	15.823	188.432	0.084	0.933
Strain SKIVE	279.644	101.765	2.748	0.007
Strain KAZ	229.568	75.489	3.041	0.003

*Supplemental Table 13*

<b>M4 Male Total SC Length</b>	<b>Estimate</b>	<b>Std. Error</b>	<b>t value</b>	<b>Pr(&gt; t )</b>
(Intercept)	1338.379	23.387	57.228	0.000
Subspecies Musculus	236.879	41.835	5.662	0.000
Subspecies Molossinus	213.996	37.502	5.706	0.000
Strain G	127.967	33.074	3.869	0.000
Strain LEW	78.836	37.502	2.102	0.040
Strain PERC	109.979	81.014	1.358	0.179
Strain PWD	3.093	44.219	0.070	0.944
Strain MSM	190.266	45.417	4.189	0.000
Strain SKIVE	-161.339	49.056	-3.289	0.002
Strain KAZ	-91.648	41.835	-2.191	0.032
Strain TOM	72.493	64.895	1.117	0.268
Strain AST	39.557	64.895	0.610	0.544

*Supplemental Table 14*

<b>M5 Male Total SC Length</b>	<b>Estimate</b>	<b>Std. Error</b>	<b>t value</b>	<b>Pr(&gt; t )</b>
(Intercept)	1338.379	23.387	57.228	0.000
Strain G	127.967	33.074	3.869	0.000
Strain LEW	78.836	37.502	2.102	0.040
Strain PERC	109.979	81.014	1.358	0.179
Strain PWD	239.972	36.041	6.658	0.000
Strain MSM	404.262	41.835	9.663	0.000
Strain MOLF	213.996	37.502	5.706	0.000
Strain SKIVE	75.540	41.835	1.806	0.076
Strain KAZ	145.230	33.074	4.391	0.000
Strain TOM	309.371	59.625	5.189	0.000
Strain AST	276.436	59.625	4.636	0.000
Strain CZECH	236.879	41.835	5.662	0.000

*Supplemental Table 15*

<b>M1 Short Bivalent SC Length</b>	<b>p values</b>		<b>Coefficients (fixed estimates)</b>	<b>Random Effects (standard deviation)</b>
Subspecies	0.12684	Intercept	80.34	
Sex	0.00000	Subspecies Musculus	-5.71	
Subspecies*Sex	0.02989	Subspecies Molossinus	-4.65	
Strain(random)	0.18840	Sex(male)	-26.26	
		Musculus*male	10.52	
		Molossinus*male		
		Intercept		2.49
		Strain		8.01

*Supplemental Table 16*

<b>M2 Short Bivalent SC Length</b>	<b>Estimate</b>	<b>Std. Error</b>	<b>t value</b>	<b>Pr(&gt; t )</b>
(Intercept)	73.886	4.633	15.947	0.000
Subspecies Musculus	6.897	6.129	1.125	0.267
Subspecies Molossinus	1.803	6.552	0.275	0.785
Strain G	7.965	5.674	1.404	0.168
Strain LEW	9.166	5.674	1.615	0.114
Strain PWD	-5.068	4.914	-1.031	0.309
Strain SKIVE	-13.897	5.674	-2.449	0.019
Sex (male)	-25.336	7.326	-3.459	0.001
Subspecies Musculus * Sex (male)	1.960	9.551	0.205	0.838
Strain G * Sex (male)	0.100	8.972	0.011	0.991
Strain LEW * Sex (male)	-2.216	9.828	-0.226	0.823
Strain PWD * Sex (male)	7.727	8.190	0.943	0.351
Strain SKIVE * Sex (male)	15.180	8.352	1.817	0.077

*Supplemental Table 17*

<b>M3 Short Bivalent SC Length</b>	<b>Estimate</b>	<b>Std. Error</b>	<b>t value</b>	<b>Pr(&gt; t )</b>
(Intercept)	73.886	4.633	15.947	0.000
Strain G	7.965	5.674	1.404	0.168
Strain LEW	9.167	5.674	1.615	0.114
Strain PWD	1.829	5.433	0.337	0.738
Strain MSM	1.803	6.552	0.275	0.785
Strain SKIVE	-7.000	6.129	-1.142	0.260
Strain KAZ	6.897	6.129	1.125	0.267
Sex (male)	-25.336	7.326	-3.459	0.001
Strain G * Sex (male)	0.100	8.972	0.011	0.991
Strain LEW * Sex (male)	-2.217	9.828	-0.226	0.823
Strain PWD * Sex (male)	9.687	9.120	1.062	0.295
Strain SKIVE * Sex (male)	17.140	9.266	1.850	0.072
Strain KAZ * Sex (male)	1.960	9.551	0.205	0.838

*Supplemental Table 18*

<b>M4 Female Short Bivalent SC Length</b>	<b>Estimate</b>	<b>Std. Error</b>	<b>t value</b>	<b>Pr(&gt; t )</b>
(Intercept)	73.886	5.334	13.853	0.000
Subspecies Musculus	6.897	7.056	0.977	0.337
Subspecies Molossinus	1.803	7.543	0.239	0.813
Strain G	7.965	6.532	1.219	0.233
Strain LEW	9.167	6.532	1.403	0.172
Strain PWD	-5.068	5.657	-0.896	0.378
Strain SKIVE	-13.897	6.532	-2.127	0.043

*Supplemental Table 19*

<b>M5 Female Short Bivalent SC Length</b>	<b>Estimate</b>	<b>Std. Error</b>	<b>t value</b>	<b>Pr(&gt; t )</b>
(Intercept)	73.886	5.334	13.853	0.000
Strain G	7.965	6.532	1.219	0.233
Strain LEW	9.167	6.532	1.403	0.172
Strain PWD	1.829	6.254	0.292	0.772
Strain MSM	1.803	7.543	0.239	0.813
Strain SKIVE	-7.000	7.056	-0.992	0.330
Strain KAZ	6.897	7.056	0.977	0.337

*Supplemental Table 20*

<b>M4 Male Short Bivalent SC Length</b>	<b>Estimate</b>	<b>Std. Error</b>	<b>t value</b>	<b>Pr(&gt; t )</b>
(Intercept)	48.550	3.120	15.563	0.000
Subspecies Musculus	12.992	4.412	2.945	0.011
Subspecies Molossinus	13.762	5.403	2.547	0.024
Strain G	8.065	3.821	2.111	0.055
Strain LEW	6.950	4.412	1.575	0.139
Strain PWD	-1.475	4.027	-0.366	0.720
Strain SKIVE	-2.852	3.821	-0.746	0.469
Strain KAZ	-4.135	4.027	-1.027	0.323

*Supplemental Table 21*

<b>M5 Male Short Bivalent SC Length</b>	<b>Estimate</b>	<b>Std. Error</b>	<b>t value</b>	<b>Pr(&gt; t )</b>
(Intercept)	48.550	3.120	15.563	0.000
Strain G	8.065	3.821	2.111	0.055
Strain LEW	6.950	4.412	1.575	0.139
Strain PWD	11.516	4.027	2.859	0.013
Strain MOLF	13.762	5.403	2.547	0.024
Strain SKIVE	10.140	3.821	2.654	0.020
Strain KAZ	8.857	4.027	2.199	0.047
Strain CZECH	12.992	4.412	2.945	0.011

*Supplemental Table 22*

<b>M4 Male Long Bivalent SC Length</b>	<b>Estimate</b>	<b>Std. Error</b>	<b>t value</b>	<b>Pr(&gt; t )</b>
(Intercept)	86.400	4.942	17.482	0.000
Subspecies Musculus	17.836	6.989	2.552	0.024
Subspecies Molossinus	11.457	8.560	1.338	0.204
Strain G	9.469	6.053	1.564	0.142
Strain LEW	9.000	6.989	1.288	0.220
Strain PWD	-3.290	6.380	-0.516	0.615
Strain SKIVE	-4.205	6.053	-0.695	0.499
Strain KAZ	-5.837	6.380	-0.915	0.377

*Supplemental Table 23*

<b>M5 Male Long Bivalent SC Length</b>	<b>Estimate</b>	<b>Std. Error</b>	<b>t value</b>	<b>Pr(&gt; t )</b>
(Intercept)	86.400	4.942	17.482	0.000
Strain G	9.469	6.053	1.564	0.142
Strain LEW	9.000	6.989	1.288	0.220
Strain PWD	14.546	6.380	2.280	0.040
Strain MOLF	11.457	8.560	1.338	0.204
Strain SKIVE	13.631	6.053	2.252	0.042
Strain KAZ	11.999	6.380	1.881	0.083
Strain CZECH	17.836	6.989	2.552	0.024

*Supplemental Table 24*

<b>M1 Normalized Foci Position</b>	<b>p values</b>		<b>Coefficients (fixed estimates)</b>	<b>Random Effects (standard deviation)</b>
Subspecies	0.124	Intercept	0.559	
Sex	0.000	Subspecies Musculus	0.009	
Subspecies*Sex	0.056	Subspecies Molossinus	0.016	
Strain(random)	0.003	Sex(male)	0.137	
		Musculus*male	-0.031	
		Molosinus*male	0.020	
		Intercept		0.019
		Strain		0.031

*Supplemental Table 25*

<b>M2 Normalized Foci Position</b>	<b>Estimate</b>	<b>Std. Error</b>	<b>t value</b>	<b>Pr(&gt; t )</b>
(Intercept)	0.590	0.018	32.808	0.000
Subspecies Musculus	-0.043	0.023	-1.907	0.061
Subspecies Molossinus	-0.016	0.024	-0.659	0.512
Strain G	-0.039	0.022	-1.753	0.085
Strain LEW	-0.051	0.021	-2.406	0.019
Strain PWD	0.028	0.017	1.653	0.103
Strain SKIVE	0.030	0.021	1.440	0.155
Sex (male)	0.142	0.023	6.251	0.000
Subspecies Musculus * Sex (male)	-0.010	0.032	-0.313	0.755
Subspecies Molossinus * Sex (male)	0.014	0.035	0.402	0.689
Strain G * Sex (male)	-0.025	0.028	-0.876	0.385
Strain LEW * Sex (male)	0.010	0.029	0.360	0.720
Strain PWD * Sex (male)	-0.040	0.028	-1.409	0.164
Strain SKIVE * Sex (male)	-0.030	0.030	-1.007	0.318

*Supplemental Table 26*

<b>M3 Normalized Foci Position</b>	<b>Estimate</b>	<b>Std. Error</b>	<b>t value</b>	<b>Pr(&gt; t )</b>
(Intercept)	0.590	0.018	32.808	0.000
Strain G	-0.039	0.022	-1.753	0.085
Strain LEW	-0.051	0.021	-2.406	0.019
Strain PWD	-0.016	0.020	-0.769	0.445
Strain MSM	-0.016	0.024	-0.659	0.512
Strain SKIVE	-0.013	0.024	-0.559	0.578
Strain KAZ	-0.043	0.023	-1.907	0.061
Sex (male)	0.142	0.023	6.251	0.000
Strain G * Sex (male)	-0.025	0.028	-0.876	0.385
Strain LEW * Sex (male)	0.010	0.029	0.360	0.720
Strain PWD * Sex (male)	-0.050	0.028	-1.765	0.082
Strain MSM * Sex (male)	0.014	0.035	0.402	0.689
Strain SKIVE * Sex (male)	-0.040	0.030	-1.343	0.184
Strain KAZ * Sex (male)	-0.010	0.032	-0.313	0.755

*Supplemental Table 27*

<b>M4 Female Normalized Foci Position</b>	<b>Estimate</b>	<b>Std. Error</b>	<b>t value</b>	<b>Pr(&gt; t )</b>
(Intercept)	0.507	0.008	64.388	0.000
Subspecies Musculus	-0.007	0.013	-0.573	0.566
Subspecies Molossinus	-0.017	0.012	-1.407	0.160
Strain G	-0.044	0.011	-3.891	0.000
Strain LEW	-0.063	0.011	-5.466	0.000
Strain PWD	-0.010	0.012	-0.868	0.385
Strain SKIVE	-0.003	0.014	-0.231	0.817

*Supplemental Table 28*

<b>M5 Female Normalized Foci Position</b>	<b>Estimate</b>	<b>Std. Error</b>	<b>t value</b>	<b>Pr(&gt; t )</b>
(Intercept)	0.507	0.008	64.388	0.000
Strain G	-0.044	0.011	-3.891	0.000
Strain LEW	-0.063	0.011	-5.466	0.000
Strain PWD	-0.018	0.010	-1.688	0.091
Strain MSM	-0.017	0.012	-1.407	0.160
Strain SKIVE	-0.010	0.013	-0.829	0.407
Strain KAZ	-0.007	0.013	-0.573	0.566

*Supplemental Table 29*

<b>M4 Male Normalized Foci Position</b>	<b>Estimate</b>	<b>Std. Error</b>	<b>t value</b>	<b>Pr(&gt; t )</b>
(Intercept)	0.733	0.014	52.208	0.000
Subspecies Musculus	-0.042	0.023	-1.827	0.076
Subspecies Molossinus	-0.142	0.021	-6.743	0.000
Strain G	-0.063	0.018	-3.611	0.001
Strain LEW	-0.040	0.020	-2.034	0.050
Strain PWD	-0.024	0.023	-1.033	0.309
Strain MSM	0.140	0.027	5.169	0.000
Strain SKIVE	-0.012	0.022	-0.541	0.592
Strain KAZ	-0.012	0.026	-0.453	0.653

*Supplemental Table 30*

<b>M5 Male Normalized Foci Position</b>	<b>Estimate</b>	<b>Std. Error</b>	<b>t value</b>	<b>Pr(&gt; t )</b>
(Intercept)	0.733	0.014	52.208	0.000
Strain G	-0.063	0.018	-3.611	0.001
Strain LEW	-0.040	0.020	-2.034	0.050
Strain PWD	-0.066	0.020	-3.303	0.002
Strain MSM	-0.001	0.026	-0.056	0.955
Strain MOLF	-0.142	0.021	-6.743	0.000
Strain SKIVE	-0.054	0.018	-2.916	0.006
Strain KAZ	-0.053	0.023	-2.334	0.026
Strain CZECH	-0.042	0.023	-1.827	0.076



*Supplemental Table 31*

<b>M1 Normalized Interfocal Distance</b>	<b>p values</b>		<b>Coefficients (fixed estimates)</b>	<b>Random Effects (standard deviation)</b>
Subspecies	0.031	Intercept	0.475	
Sex	0.000	Subspecies Musculus	0.006	
Subspecies*Sex	0.047	Subspecies Molossinus	-0.003	
Strain(random)	0.244	Sex(male)	0.069	
		Musculus*male	0.052	
		Molossinus*male	-0.008	
		Intercept (strain)		0.009
		Strain (residual)		0.048

*Supplemental Table 32*

<b>M2 Normalized Interfocal Distance</b>	<b>Estimate</b>	<b>Std. Error</b>	<b>t value</b>	<b>Pr(&gt; t )</b>
(Intercept)	0.461	0.023	19.812	0.000
Subspecies Musculus	0.021	0.031	0.659	0.512
Subspecies Molossinus	0.003	0.048	0.061	0.952
Sex (male)	0.082	0.031	2.619	0.011
Strain G	0.027	0.030	0.892	0.375
Strain LEW	0.012	0.028	0.432	0.667
Strain PWD	-0.002	0.026	-0.073	0.942
Strain MSM	0.009	0.036	0.247	0.806
Strain SKIVE	0.000	0.031	0.010	0.992
Subspecies Musculus * Sex (male)	-0.043	0.046	-0.934	0.354
Subspecies Molossinus * Sex (male)	-0.016	0.047	-0.338	0.736
Strain G * Sex (male)	-0.029	0.040	-0.739	0.462
Strain LEW * Sex (male)	0.000	0.041	-0.007	0.995
Strain PWD * Sex (male)	0.085	0.043	1.993	0.050
Strain SKIVE * Sex (male)	0.121	0.045	2.699	0.009

*Supplemental Table 33*

<b>M3 Normalized Interfocal Distance</b>	<b>Estimate</b>	<b>Std. Error</b>	<b>t value</b>	<b>Pr(&gt; t )</b>
(Intercept)	0.461	0.023	19.812	0.000
Sex (male)	0.082	0.031	2.619	0.011
Strain G	0.027	0.030	0.892	0.375
Strain LEW	0.012	0.028	0.432	0.667
Strain PWD	0.019	0.028	0.668	0.506
Strain MSM	0.012	0.033	0.357	0.722
Strain MOLF	-0.013	0.031	-0.418	0.678
Strain SKIVE	0.021	0.033	0.635	0.528
Strain KAZ	0.021	0.031	0.659	0.512
Strain G * Sex (male)	-0.029	0.040	-0.739	0.462
Strain LEW * Sex (male)	0.000	0.041	-0.007	0.995
Strain PWD * Sex (male)	0.042	0.041	1.038	0.303
Strain MSM * Sex (male)	-0.016	0.047	-0.338	0.736
Strain SKIVE * Sex (male)	0.078	0.043	1.821	0.073
Strain KAZ * Sex (male)	-0.043	0.046	-0.934	0.354

*Supplemental Table 34*

<b>M4 Female Normalized Interfocal Distance</b>	<b>Estimate</b>	<b>Std. Error</b>	<b>t value</b>	<b>Pr(&gt; t )</b>
(Intercept)	0.461	0.026	18.066	0.000
Subspecies Musculus	0.021	0.034	0.601	0.552
Subspecies Molossinus	0.012	0.036	0.325	0.747
Strain G	0.027	0.033	0.814	0.422
Strain LEW	0.012	0.031	0.394	0.696
Strain PWD	-0.002	0.028	-0.067	0.947
Strain SKIVE	0.000	0.034	0.009	0.993

*Supplemental Table 35*

<b>M5 Female Normalized Interfocal Distance</b>	<b>Estimate</b>	<b>Std. Error</b>	<b>t value</b>	<b>Pr(&gt; t )</b>
(Intercept)	0.461	0.026	18.066	0.000
Strain G	0.027	0.033	0.814	0.422
Strain LEW	0.012	0.031	0.394	0.696
Strain PWD	0.019	0.031	0.609	0.546
Strain MSM	0.012	0.036	0.325	0.747
Strain SKIVE	0.021	0.036	0.579	0.567
Strain KAZ	0.021	0.034	0.601	0.552

*Supplemental Table 36*

<b>M4 Male Normalized Interfocal Distance</b>	<b>Estimate</b>	<b>Std. Error</b>	<b>t value</b>	<b>Pr(&gt; t )</b>
(Intercept)	0.543	0.019	29.268	0.000
Subspecies Musculus	-0.017	0.030	-0.564	0.576
Subspecies Molossinus	-0.013	0.028	-0.469	0.642
Strain G	-0.003	0.023	-0.110	0.913
Strain LEW	0.012	0.026	0.459	0.649
Strain PWD	0.078	0.030	2.573	0.014
Strain MSM	0.009	0.032	0.277	0.783
Strain SKIVE	0.116	0.029	4.046	0.000
Strain KAZ	-0.005	0.034	-0.160	0.874

*Supplemental Table 37*

<b>M5 Male Normalized Interfocal Distance</b>	<b>Estimate</b>	<b>Std. Error</b>	<b>t value</b>	<b>Pr(&gt; t )</b>
(Intercept)	0.543	0.019	29.268	0.000
Strain G	-0.003	0.023	-0.110	0.913
Strain LEW	0.012	0.026	0.459	0.649
Strain PWD	0.061	0.026	2.320	0.026
Strain MSM	-0.004	0.030	-0.140	0.889
Strain MOLF	-0.013	0.028	-0.469	0.642
Strain SKIVE	0.099	0.024	4.065	0.000
Strain KAZ	-0.022	0.030	-0.743	0.462
Strain CZECH	-0.017	0.030	-0.564	0.576

*Supplemental Table 38*

<b>M1 Raw Interfocal Distance</b>	<b>p values</b>		<b>Coefficients (fixed estimates)</b>	<b>Random Effects (standard deviation)</b>
Subspecies	0.128	Intercept	57.461	
Sex	0.026	Subspecies Musculus	-0.713	
Subspecies*Sex	0.084	Subspecies Molossinus	2.932	
Strain(random)	0.409	Sex(male)	-6.68	
		Musculus *male	7.364	
		Molossinus*male	-4.536	
		Intercept (strain)		0
		Strain (residual)		7.78

*Supplemental Table 39*

<b>M2 Raw Interfocal Distance</b>	<b>Estimate</b>	<b>Std. Error</b>	<b>t value</b>	<b>Pr(&gt; t )</b>
(Intercept)	53.713	3.788	14.179	0.000
Subspecies Musculus	8.732	5.082	1.718	0.090
Subspecies Molossinus	4.038	7.886	0.512	0.610
Sex (male)	-5.769	5.082	-1.135	0.260
Strain G	6.534	4.890	1.336	0.186
Strain LEW	3.532	4.639	0.761	0.449
Strain PWD	-6.918	4.226	-1.637	0.106
Strain MSM	2.642	5.786	0.457	0.649
Strain SKIVE	-10.073	5.082	-1.982	0.052
Subspecies Musculus * Sex (male)	-8.650	7.513	-1.151	0.254
Subspecies Molossinus * Sex (male)	-3.938	7.701	-0.511	0.611
Strain G * Sex (male)	-2.717	6.463	-0.420	0.676
Strain LEW * Sex (male)	0.376	6.670	0.056	0.955
Strain PWD * Sex (male)	18.610	6.962	2.673	0.009
Strain SKIVE * Sex (male)	21.876	7.291	3.000	0.004

*Supplemental Table 40*

<b>M3 Raw Interfocal Distance</b>	<b>Estimate</b>	<b>Std. Error</b>	<b>t value</b>	<b>Pr(&gt; t )</b>
(Intercept)	53.713	3.788	14.179	0.000
Sex (male)	-5.769	5.082	-1.135	0.260
Strain G	6.534	4.890	1.336	0.186
Strain LEW	3.532	4.639	0.761	0.449
Strain PWD	1.814	4.553	0.398	0.692
Strain MSM	6.680	5.357	1.247	0.217
Strain MOLF	0.100	5.082	0.020	0.984
Strain SKIVE	-1.341	5.357	-0.250	0.803
Strain KAZ	8.732	5.082	1.718	0.090
Strain G * Sex (male)	-2.717	6.463	-0.420	0.676
Strain LEW * Sex (male)	0.376	6.670	0.056	0.955
Strain PWD * Sex (male)	9.960	6.610	1.507	0.137
Strain MSM * Sex (male)	-3.938	7.701	-0.511	0.611
Strain SKIVE * Sex (male)	13.226	6.956	1.902	0.062
Strain KAZ * Sex (male)	-8.650	7.513	-1.151	0.254